

Deciphering Connections Between the Microbial Communities of the Euphotic Zone and
Sinking Particles in the Sargasso Sea

by

Marc Alec Fontáñez Ortiz

A Thesis Presented in Partial Fulfillment
of the Requirements for the Degree
Master of Science

Approved July 2022 by the
Graduate Supervisory Committee:

Susanne Neuer, Chair
Qiyun Zhu
Elizabeth Trembath-Reichert

ARIZONA STATE UNIVERSITY

August 2022

ABSTRACT

Sinking particles are important conduits of organic carbon from the euphotic zone to the deep ocean and microhabitats for diverse microbial communities, but little is known about what determines their origin and community composition. Events in the northwestern Sargasso Sea such as winter convective mixing, summer stratification, and mesoscale (10–100 km) eddies, characteristic features of this region, affect the vertical and temporal composition and abundance of pelagic and particle-attached microorganisms. To assess the connections of the microbial communities between the euphotic zone and sinking particles, I carried out indicator and differential abundance analyses of prokaryotes and photoautotrophs based on the V4-V5 amplicons of the 16S rDNA from samples collected in the Sargasso Sea during the spring and summer of 2012. I found that gammaproteobacteria such as *Pseudoalteromonas* sp. and *Vibrio* sp., common particle-associated bacteria often linked with zooplankton, dominated the sequence libraries of the sinking particles. The analysis also revealed that members of *Flavobacteria*, particularly the fish pathogen *Tenacibaculum* sp., as well as *Chloropicon* sp. and *Chloroparvula* sp., among the smallest known green algae, were indicators taxa of sinking particles. The cryptophyte *Teleaulax* and the diatom *Chaetoceros* were overrepresented in the particle communities during both seasons. Interestingly, I also found that the large centric diatom, *Rhizosolenia* sp., generally rare in the oligotrophic Sargasso Sea, dominated photoautotrophic communities of sinking particles collected in the center of an anticyclonic eddy with unusual upwelling due to eddy-wind interactions. I hypothesize that the steady contribution by picophytoplankton to particle flux is punctuated by pulses of production and flux of larger-sized phytoplankton

in response to episodic eddy upwelling events and can lead to higher export of particulate organic matter during the summer.

DEDICATION

«¡Que Dios me lo bendiga y la virgen me lo favorezca!»

Así comenzaban todas mis mañanas. El café no podía faltar para que mi abuela, mi madre y yo nos contáramos todos nuestros sueños antes de comenzar el día. Nuestra vida era una paradoja—nos faltó de todo y al mismo tiempo, nada. Abuela, recuerdo cuando me acobijabas bajo tus brazos mientras nos mesías en la hamaca.

«¡Mami, hazme el cuento!»

Sabías muy bien que quería el *Cuento del mamey*. El final era mi parte favorita, porque siempre terminábamos muertos de la risa.

Hoy día tienes 102 años, y agradecido estoy con la vida de que todavía me puedas hacer el cuento. A ti, mi amadísima abuela, te dedico este trabajo, aunque haya sido el tiempo que me costó, lo que hubiese querido dedicarte. Hoy quedo en desasosiego, puesto que, la demencia senil, poco a poco se ha llevado la luz de tus ojos. Pero, esos hoyuelos, los que tú y yo compartimos, siempre quedarán marcados en mi corazón. Te amo, te extraño, y gracias por todo.

ACKNOWLEDGMENTS

I belong in science—that has been the central theme of my graduate journey. Herein, I express my overwhelming gratitude to the people who, one way or another, influenced this realization and ushered my convoluted path to becoming a microbial oceanographer. My gratitude starts with my participation in an internship at Woods Hole Oceanographic Institution. At the time, I didn't have a clear idea of what I wanted to pursue—fortunately, the dedication and motivation from Drs. Julie Huber and Elizabeth Trembath-Reichert, and that from the Partnership Education Program, helped me find my calling in microbial oceanography.

As a master's student, I became part of Dr. Susanne Neuer's Lab. She took in a student with great motivation but also one struggling to understand how much he belongs in science. Therefore, Susanne was pivotal in catapulting my career as a microbial oceanographer and, with that, my confidence. With her advisership, I was able to extend my scientific network and conduct research at the Bermuda Institute of Ocean Sciences, where I embarked on three research cruises and became instrumental in our field experiments at the Sargasso Sea.

The colleagues and friends I made along the way were influential in my scientific development, two of which served as role models and still resonate strongly today. First, I want to give a special thanks to Dr. Steffen Buessecker for being inspirational in my career and always making me feel welcome. His thoughtfulness and dedication to the students helped me confidently engage in geochemical techniques. But more importantly, in him, I found a friend with whom I can confide and share a cultural experience. Second, I want to thank Dr. Bianca Nahir Cruz for always finding time to navigate scientific questions with

me. I cherish the many conversations we had in which we brainstormed, and the times we talked about our struggles. Thank you both for believing in me.

I thank my graduate committee, Drs. Qiyun Zhu and Elizabeth Trembath-Reichert, for being instrumental in helping me develop the skills needed to tackle this thesis. The foundation of my knowledge in amplicon sequence analysis was thanks to their dedicated effort. I also thank the School of Life Sciences, the Graduate Office, and the Microbiology *Program Director*, Dr. Rajeev Misra, for nominating me to receive the SOLS MS Award. This award funded part of my degree and supported the necessary research to finish my thesis. I do not think it would have been economically possible without this help.

I thank my friends, Steven J. Toro De León and Mahmoud Matar Abed. We started our journey as undergrads in Puerto Rico, exploring what it meant to be a scientist. Now we are all successfully pursuing graduate studies and following our dreams. Our virtual gatherings, where we support each other, learn about financial literacy, and even about philosophical points of view, serve as motivation to strive and continue strong. I am incredibly thankful for our friendship, which defines space and time. Finally, I thank my mother, Lorraine Ortiz Concepción, who showed me how to be resilient in adversity, my grandmother, Emilia Concepción González, who showed me how to be ambitious and optimistic, and my brother, Marlon M. Fontáñez Ortiz, whose ingenuity, and curiosity influence my own during our upbringing. Without the support of my family, I would not have had the strength to pursue my career. My love and gratitude towards them are unconditional and indescribable.

—Thank you all for enlightening my path to what today has become my passion—

TABLE OF CONTENTS

	Page
LIST OF TABLES	vi
LIST OF FIGURES	vii
INTRODUCTION	1–5
MATERIALS AND METHODS	5–12
Sample Collection and Processing	5–6
DNA Extraction, 16S rRNA Gene Amplification, Sequencing and Analysis	6–8
Statistical Analyses	8–12
RESULTS	12–21
Hydrographical Settings.....	12–13
Prokaryotes	13–18
Photoautotrophs.....	18–21
DISCUSSION	21–35
Community Structure as Evidence of Complex Microbial Interactions	23–29
Phototrophic Community of Large Diatoms Dominate Particle Export	30–34
Contributions of Picophytoplankton to Particle Export.....	35
REFERENCES	36–49
APPENDIX	
A TABLES	50–56
B FIGURES	57–66

LIST OF TABLES

Table	Page
1. Sampling Dates and Station Locations	51
2. Sample Information, Sequence Counts and Alpha-Diversity Measures	52
3. PERMANOVA based on Bray-Curtis Dissimilarity of Prokaryotes	53
4. PERMANOVA based on Bray-Curtis Dissimilarity of Photoautotrophs	54
5. Indicator Species Analysis for Prokaryotes	55
6. Indicator Species Analysis for Photoautotrophs	56

LIST OF FIGURES

Figure	Page
1. Prokaryote Species-Saturation Curves	58
2. Photoautotroph Species-Saturation Curves	58
3. Heatmap and Dendrogram of Compositional Dissimilarity of Prokaryotes	59
4. NMDS of Bray-Curtis Compositional Difference of Prokaryotes	60
5. Alpha-diversity Violin-Box Plot for Prokaryotes	60
6. Ballon plot of Prokaryotic Indicator Taxa in Trap Material	61
7. Differential Abundance Analysis of Prokaryotes in Spring and Summer	62
8. Heatmap and Dendrogram of Compositional Dissimilarity of Prokaryotes	63
9. NMDS of Bray-Curtis Compositional Difference of Prokaryotes	64
10. Alpha-diversity Violin-Box Plot for Prokaryotes	64
11. Ballon plot of Prokaryotic Indicator Taxa in Trap Material	65
12. Differential Abundance Analysis of Prokaryotes in Spring and Summer	66

INTRODUCTION

Oligotrophic gyres are the ocean's desert. They comprise 40% of the Earth's surface (Polovina et al., 2008) and are characterized by low productivity, low phytoplankton biomass and small-sized phytoplankton (generally $<5 \mu\text{m}$) relative to eutrophic areas (Dortch & Packard, 1989; Fernández-Castro et al., 2012). Nevertheless, the Sargasso Sea experiences annual deep convective mixing during the winter (Cianca et al., 2012; Palter et al., 2005), therefore, deepening the mixed layer with depths ranging from 100 to 400 m (Lomas et al., 2013). This mixing with nutrient-rich water from below (Steinberg et al., 2001) also causes relaxation of grazing pressure on the phytoplankton community due to dilution of the protistan grazers (Treusch et al., 2012). This results in higher phytoplankton biomass and "new" primary production, leading to the winter-spring bloom (Helmke et al., 2010; Fernández-Castro et al., 2012; Lomas et al., 2013).

Mesoscale eddies are another physical forcing mechanism that can affect plankton communities in the Sargasso Sea (McGillicuddy & Robinson, 1997; McGillicuddy, 2016). Eddies are rotating water masses that propagate westward in the North Atlantic (Gaube et al., 2018; Richardson, 1983) and can introduce spatial heterogeneity and variability across scales of 10 to 100 kilometers (Sweeney et al., 2003). These vortices can be characterized by three different displacements of the seasonal thermocline that can either promote upwelling (cyclones and mode-water eddies) or downwelling (anticyclones) depending on their direction of rotation, or inclusion of lenses of eighteen degree water (Mouriño-Carballido & Sweeney et al., 2003; McGillicuddy, 2006; Mouriño-Carballido, 2009). Cyclones rotate counterclockwise and uplift the nutricline into the euphotic zone (McGillicuddy & Robinson, 1997). Anticyclones rotate clockwise and act opposite to

cyclones by deepening the depth of the seasonal thermocline and pushing nutrient-rich waters deeper (McGillicuddy, 2015). Mode-water eddies are similar to cyclones in that they promote upwelling (Bibby et al., 2008) but rotate clockwise, similar to anticyclones (Sweeney et al., 2003). Moreover, mode-water eddies produce an upward displacement of the seasonal thermocline and a downward displacement of the permanent thermocline, creating intra-thermocline lenses (McGillicuddy, 2015). All eddies have a surface signature by either slightly uplifting or lowering the sea-surface (Pascual et al., 2006; Nian et al., 2021) and can be localized by altimetry satellites (Holloway, 1986; Mason et al., 2014). The effect of mesoscale eddies on primary production can also vary within the same feature. While the impact of eddies on primary production is usually more pronounced at the core, their edges can have different effects on the plankton community, as well as interactions between adjacent eddies (Sweeney et al., 2003). Furthermore, young eddies (< 4 months) usually show a stronger biological response compared to older ones (Mouriño-Carballido, 2009; Sweeney et al., 2003). Mesoscale eddies can exert more influence on primary productivity than the seasonality of mixing and stratification explained above (Helmke et al., 2010; K. Richardson & Bendtsen, 2017). Therefore, there is an interest in correctly portraying eddy behavior and its effect on the phytoplankton community in climate models (e.g., TRR 181 Energy transfer in Atmosphere and Ocean).

Picophytoplankton (0.2-2 μm) are the most abundant primary producers in oligotrophic regions (Scanlan et al., 2009; Stockner, 1988). Within this phytoplankton size class, two cyanobacteria genera dominate the Sargasso Sea, *Prochlorococcus* and *Synechococcus* (De Martini et al., 2018). They can thrive in nutrient-poor environments due to their high surface-to-volume ratios (Partensky et al., 1999; Lavallée & Pick, 2002)

and adaptations for efficient nutrient acquisition in oligotrophic systems (Moore et al., 2005; Ustick et al., 2021). While *Prochlorococcus* usually co-occurs with *Synechococcus* between 40°N and 40°S, they experience different ecological patterns (Flombaum et al., 2020). *Prochlorococcus* presents a strong vertical partitioning under stratified conditions represented as distinct ecotypes (Mella-Flores et al., 2012), a high-light ecotype with low chlorophyll *b/a* ratios adapted to higher light intensities and a low-light ecotype with high chlorophyll *b/a* ratios adapted to extremely low irradiance found in the deeper regions of the euphotic zone (Rocap et al., 2002). In contrast, *Synechococcus* does not show vertical partitioning but rather a strong diversification that optimizes its ability to manage short-term changes in nutrient availability in the euphotic zone (Sohm et al., 2016). Picoeukaryotes are also adapted to oligotrophic environments but have a lower abundance than the picocyanobacteria in the water column relative to the total phytoplankton biomass in the Sargasso Sea (DuRand et al., 2001).

Through photosynthesis, phytoplankton fix dissolved inorganic carbon into organic matter, playing a key role in the global carbon cycle and in carbon export (Neuer et al., 2002). The Biological Carbon Pump leads the large-scale export of organic matter to the dark ocean (Neuer et al., 2014; Flintrop et al., 2018). Organic matter is exported mainly as particulate organic carbon by the gravitational sinking of particles (Boyd et al., 2019; Buesseler et al., 2020). The export of the particles out of the euphotic zone depends on their composition, size, and density, which determine their sinking velocity (Iversen & Lampitt, 2020), as well as the biological processes that recycle and degrade the sinking particles (Ducklow et al., 2001). Marine particle aggregation is mediated by sticky exopolymeric substances that phytoplankton and bacteria exude, some of which coagulate

to form gels. One type of these gels is transparent exopolymer particles or TEP (Passow, 2002; Cruz & Neuer, 2019) made up of charged acidic polysaccharides (Villacorte et al., 2015; Chen et al., 2021) that are abundantly present in the ocean and can interact with other surfaces (Verdugo, 2012). The collision of marine aggregates with biogenic and lithogenic ballasting minerals and zooplankton fecal pellets can also enhance the particle's composition. Zooplankton plays an important role in the biological carbon pump (Cruz et al., 2021); they either prey on phytoplankton or "repackage" marine particles (Baumas et al., 2021), producing fecal pellets that can sink or interact with other marine particles, therefore, contributing to the Particulate Organic Carbon (POC) flux. Moreover, heterotrophic bacteria are contained in and colonize the particles (Grossart et al., 2006), which enhance aggregation by promoting TEP production and increasing particle stickiness (Cruz et al., 2019). Hence, marine particles serve as microhabitats for diverse microbial communities whose abundance is 3-5 log-fold higher than surrounding seawater (Datta et al., 2016; Rogge et al., 2018). Bacteria in marine aggregates can promote fast particulate organic matter turnover (Suttle et al., 1991; Tansel, 2018) and therefore play an essential role in the degradation of aggregates as they are exported to depth (Omand et al., 2020). The carbon export can be measured using surface-tethered Particle Interceptor Traps (PITs) that collect the sinking particles (Knauer et al., 1978) and allow the quantification of POC export.

In this study, I investigate what processes drive the composition of the eukaryotic and prokaryotic microbial communities in the euphotic zone and those on sinking particles collected below the euphotic zone in the Sargasso Sea. I carried out this investigation in the winter/spring and summer seasons, while targeting different mesoscale eddies. This study

adds to earlier work (Cotti-Rausch et al., 2016, 2020; De Martini et al., 2018) that investigated the influence of mesoscale features and seasons on the composition, production and export of the plankton community in the oligotrophic Sargasso Sea.

MATERIALS AND METHODS

Sample collection and processing

The investigation was carried out on the *R/V Atlantic Explorer* in the spring and summer of 2012, as described by De Martini et al. (2018) and Cotti-Rausch et al. (2016, 2020). In spring 2012, the center of a 6-month-old cyclonic eddy (C2) and the Bermuda Atlantic Time-series Study (BATS) site were sampled. In July 2012, samples were collected from the center and the edge of a < 1-month-old anticyclonic eddy (AC2, ACe2) as well as from BATS, influenced by the edge of a cyclonic eddy. All stations were sampled twice, 48 h apart (Table 1).

Seawater samples were collected at the four sites to analyze the DNA of the free-living microbial community using 12 L Niskin bottles mounted on a CTD-rosette (SBE9/11+; Sea Bird Electronics) deployed at 20 m and the deep-chlorophyll maximum (DCM; Table 2). Two liters were collected per depth, filtered onto GF/F (0.7 μm Whatman; GE Healthcare), which were placed in 1.5 mL cryovial tubes, flash-frozen in liquid N_2 , and stored at -80°C until processing. A three-day deployment of poisoned surface-tethered Particle Interceptor Traps (PITs) was done at the four sites (Table 1) to study the microbial community associated with sinking particles below the euphotic zone at 150 m depth. Briefly, the PITs array was fitted with acid-washed (10% HCl) 0.8 μm polycarbonate membrane filters at the bottom of each tube and filled with poisoned seawater brine (0.74%

formalin final concentration; ca. 50g NaCl L⁻¹ above ambient salinity), according to BATS standard protocols (Knap et al., 1997; <http://bats.bios.edu/>). Upon recovery, the caps and baffles from each tube were removed to siphon off the seawater that entered above the density layer of the poisoned brine. The remaining dense layer was left to filter through the membrane by opening the valve at the bottom. During this process, the caps for the tubes were placed back loosely to avoid ambient particles from entering the samples. After filtration, membranes were carefully removed from the tubes and placed onto acid-washed (10% HCl) glass Petri dishes to remove any swimmers (zooplankton; Knap et al., 1997; Buesseler et al., 2007; <http://bats.bios.edu/>) using sterile (70% EtOH) forceps and a dissection microscope on the ship. The particulate material attached to the membrane of each trap cone was rinsed with sterile-filtered seawater (0.2 µm/0.2 µm AcroPak 1000; Pall Corp) onto a 25 mm GF/F filter using a vacuum filtration system with cone-shaped funnels. The GF/F filters were placed in 1.5 mL cryovial tubes and immediately flash-frozen in liquid N₂. Upon docking, cryovials containing the seawater and trap material were transported to ASU in a dry shipper and stored at -80°C until later processing. Replicate tubes were analyzed from each deployment.

DNA extraction, 16S rRNA gene amplification, sequencing, and analyses

The DNA of euphotic zone and trap samples was extracted using a QIAGEN DNeasy Blood and Tissue Kit (De Martini et al., 2018). 16S rRNA gene amplicon libraries were prepared and sequenced using an Illumina MiSeq platform (reagent kit v3; 2x300bp paired-end; Illumina Inc.) by the Dalhousie University Integrated Microbiome Resource (IMR) using the universal V4 and V5 primer set: 515F-Y (5'-

GTGYCAGCMGCCGCGGTAA-3'; Parada et al., 2016) and 926-R (5'-CCGYCAATTYMTTTRAGTTT-3'; Quince et al., 2011; Parada et al., 2016).

The demultiplexed reads received from IMR were analyzed using QIIME2 (v2021.4). After importing the FASTQ files, the quality scores were assessed to choose a median above 30, positioned before the sharp decrease in read quality. Primers were then trimmed using the QIIME2 plugin (q2-plugin) *cutadapt*. Amplicon Sequence Variants (ASVs) were prepared from the trimmed reads with the q2-plugin *DADA2*. Different sequence base positions were compared as truncation parameters to ensure sufficient read recovery during the denoising step. The best non-chimeric recovery was obtained at ca. 70% for most samples using position 243 in forward reads and 166 in reverse reads using a minimum overlap of 12 bases between the forward and reverse reads. The resulting ASVs were classified using the SILVA database (v138.1; Quast et al., 2013) for the 16S rRNA reads of prokaryotes and the PR² database (v14.4; Guillou et al., 2013), which includes PhytoREF as of April 2021 for the photoautotrophic taxa. Before classifying the prokaryotes with SILVA, the database was pre-processed using the q2-plugin *RESCRIPt* to ensure a standardized processing before training the classifier with the V4-V5 primer set (Robeson et al., 2021). The same was not valid for PR² as *RESCRIPt* does not work for this database. Classified ASV tables were filtered from taxa identified as contaminants from the environmental blank. This blank was not prepared for the extraction session but rather for the aliquoting process as preparation for the sequencing facility. In addition, the mitochondria, chloroplasts, and unassigned sequences from the SILVA-classified ASV table were removed, while the PhytoREF/PR²-classified ASV table was filtered only to contain 16S rRNA gene sequences from plastids and cyanobacteria, and without filtering

unknown bacterial sequences. The ASV counts per sample from the filtered tables were used along with alpha-rarefaction plots to assess the sampling depth for rarefaction (Figures 1–2). Seawater samples had higher sequence depths compared to particle trap material; therefore, I adjusted differences in library size across samples by rarefying to the smallest sample size using a minimum of ca. 1,000 sequences per sample for each dataset. Due to this adjustment, three samples were lost in both datasets: a trap sample collected from BATS spring 2012, a seawater sample collected from 20 m depth in AC2 summer 2012, and a trap sample collected from BATS summer 2012 (Table 2).

Statistical Analysis

Median values from alpha-diversity metrics of even sampling depths were calculated using non-rarefied ASV tables through the q2-plugin *alpha-rarefaction* and applying 25 iterations. The maximum depth used for even sampling was a value equal to or less than the median sample depth. I used *Observed Features* to assess richness, and *Shannon's Index* for diversity as the alpha-rarefaction metrics (options found within *alpha-rarefaction*). The median values calculated from *alpha-rarefaction* were plotted using functions within the *ggplot2* (v 3.3.5) and *reshape* (v 0.8.8) packages in R statistical software (v 4.0.5). Further statistical modeling was done using the rarefied taxa tables.

Diversity metrics were subject to visual inspection of data normality via histograms, and statistical inspection by applying the Shapiro-Wilk test. The homogeneity of variances of the residues was verified by a Leven's test. Given that not all data showed a normal distribution, non-parametric assumptions were applied, and the Kruskal-Wallis *H* test was used to determine if there was a significant difference of medians between the

predetermined groups. The groups contained alpha diversity metrics calculated from the q2-plugin *diversity alpha*, which gives a single numeric value for each sample. The metrics were grouped by depth (20m, DCM and 150 m) and separated by season (spring and summer). Pairwise comparisons were done by applying the Dunn's Multiple Comparisons *post hoc* test (Dunn, 1961). This test allowed the identification of significant differences among the groups. To decrease the probability of false discovery rate (FDR), the p-values were adjusted using the Benjamini-Hochberg method, therefore controlling for Type I errors (Verhoeven et al., 2005). Alpha-diversity metrics were plotted as violin plots overlaid to box and whiskers plots to assess group significance, distribution, and variation among sample groups. The *ggbetweenstats* function from the *ggstatsplot* package (v 0.9.1) in R was used to run the statistical analysis using non-parametric assumptions and to simultaneously create the plots. For reproducibility, the same eight random values were repeatedly used as seed in every statistical analysis within R that required randomization.

A distance matrix was computed using Bray-Curtis dissimilarities from the $\log(X + 1)$ -transformed relative abundance of each rarefied table to create a heatmap. This transformation allows better represent datasets with a right-skewed frequency due to sparsity by adding a pseudocount. A hierarchical clustering analysis was performed using the Unweighted Pair Group Method with Arithmetic Mean (UPGMA) along with a Similarity Profile Routine (SIMPROF) to determine significant differences between the clusters (999 iterations; 5% significance level). These statistical analyses and visualization (dendrogram overlaid to a heatmap) were performed using PRIMER-E (v7; Clarke & Gorley, 2015). Further statistical modeling was performed within R statistical software (v 4.0.5) by creating an R object of the rarefied tables using the *phyloseq* package (v 1.34.0).

The rarefied taxa tables were used to prepare a non-metric multidimensional scaling (NMDS) ordination based on Bray-Curtis dissimilarity distances. The differences associated with sample types (seawater and trap material), season (spring and summer) as well as depth (20 m, DMC, and 150 m) were visualized. A Pairwise Permutational Multivariate Analysis (PERMANOVA; Anderson, 2001) was performed within the *metaMDS* and *adonis* functions from the *vegan* (v2.5-7) package using the same factors from the NMDS. To decrease the probability of falsely rejecting the null hypothesis due to multiple comparisons, the *FDR* method (Verhoeven et al., 2005) was implemented using the base R function, *p.adjust*.

To determine the strength of associations between the taxa and *a priori* groups (seawater and particulate trap material), the indicator value (IndVal) was calculated using group combinations with the *multipatt* function from the *indicspecies* package (v 1.7.9; De Cáceres et al., 2010). This analysis used the relative abundance and occurrence to identify the *fidelity* and *specificity* of each taxon to either or both seawater and particulate trap material using the rarefied table and by applying the following equation:

$$IndVal_{ij} = \sqrt{100(A_{ij} * B_{ij})}$$

Where A_{ij} is the specificity, i.e., the abundance of species i in group j , and B_{ij} is the fidelity, i.e., frequency by which species i appears in group j . IndVal is highest when taxa are exclusively found in one of the *a priori* groups while expressing high relative abundance within that same group (Severns & Sykes, 2020). A Monte Carlo permutational

test ($n_{\text{perm}} = 9999$) was also added using the *how* function from the *indicspecies* dependency, *permute* (v 1.9-5). This function helped to assess the statistical significance of each individual indicator value. To report the group-wise indicator values, the *p-value* was adjusted for multiple testing issues, as advised by De Cáceres et al. (2010), using the Benjamini-Hochberg procedure (Benjamini & Hochberg, 1995) only taxa with an adjusted $p \leq 0.05$ were chosen.

To identify the taxa that drive the community difference between seawater and particle trap material in both seasons, a differential abundance analysis was performed using the *DESeq2* package (v 1.35.0). This analysis first estimates size factors to avoid a library composition bias by dividing the raw counts by the geometric means of each taxon. Raw counts are then divided by the median of the size factors of each sample. The package then estimates dispersions for each ASV using the Maximum Likelihood Estimation, fits a curve to ASV-wise dispersion estimates, and shrinks these estimates towards the values predicted by the negative binomial distribution. Finally, it fits a generalized linear model, performs hypothesis testing, and generates a list of differentially abundant ASVs. Before running the analysis, the *phyloseq* object was first transformed by pruning samples that were not part of the groups of interest (e.g., removing summer samples when analyzing spring samples) to ensure the correct calculation of the geometric means. Next, the hypothesis testing was done using the Wald test for a two-group comparison (Wald, 1943), and the *p-value* was adjusted using the Benjamini-Hochberg procedure (FDR; Verhoeven et al., 2005). The taxa with a significant (FDR-correct $p < 0.05$) \log_2 -fold change (L2FC) difference between seawater and particle trap material from one specific season were

plotted. Finally, the plots were color-coded with the relative percent abundance calculated from the normalized mean counts of the samples relative to the targeted season comparison.

RESULTS

Hydrographical settings:

This study is part of the Trophic-BATS project that aims to shed light on the trophic interactions within the euphotic zone and their connection to carbon export in the oligotrophic Sargasso Sea (Cotti-Rausch et al., 2016; De Martini et al., 2018). This study explores plankton community export, focusing on the prokaryotic and autotrophic assemblages within the euphotic zone and particulate trap samples. The Sargasso Sea is characterized by strong meridional gradients (Siegel, 1990; Sweeney et al., 2003), having seasonal mixing events in the northernmost part and permanent stratification in the south (Cianca et al., 2012; Nelson et al., 2004). This study's location lies near the center of this gradient, where mesoscale eddies have been suggested as important and dominant features that induce biological responses by producing upwelling events in the upper ocean (Cianca et al., 2012; McGillicuddy et al., 2001). During the sampling, cold-core (cyclonic) and warm-core (anticyclonic) mesoscale eddies in the vicinity of BATS during early spring and mid-summer 2012 were targeted. Cotti-Rausch et al. (2016) provide detailed descriptions of these features. Briefly, during spring 2012, a 6-month-old cyclonic eddy (C2) northeast of BATS presented a cold-core (19.5°C) and low-nutrient inventories, but a deeper mixed layer depth (~150 m) compared to BATS (20.5°C; MLD 65–135 m), which was not eddy-influenced. While the slightly colder temperatures at the core compared to BATS are evidence of an upwelling event (Andersen et al., 2011; Sweeney et al., 2003), the lower

nutrient inventory in the cyclone suggests it was a decaying feature or that there was low mixing from outside of the eddy (Cotti-Rausch et al., 2016; Mouriño-Carballido & McGillicuddy, 2006). In the summer of 2012, the center and edge of a less than a month-old anticyclonic eddy (AC2) northwest of BATS (Cotti-Rausch et al., 2016; De Martini et al., 2018) presented upwelling caused by eddy/wind interactions (McGillicuddy et al., 2007). All stations showed temperatures ranging from 28°C at the surface to 20°C at the base of the euphotic zone and shallow mixed layers, with the shallowest depth being at BATS (15–22 m), followed by the center (18–24 m) and edge (25–34 m) of the anticyclone. BATS was influenced by the edge of a young cyclone located southeast of the site (see Fig. 1 in De Martini et al., 2018).

In the following sections, I present the amplicon analysis results of both prokaryotes and plastid ASVs by disentangling seasonal differences influenced by mesoscale eddies in the oligotrophic Sargasso Sea. I first explore the *community composition and diversity* to identify the taxa associated with the euphotic zone and those predominantly found in sinking particles. Thereafter, I identify the *drivers of community differences* between the water column and the shallow trap samples by measuring the strength of associations of individual taxa and their differential abundance within the samples relative to the season.

Prokaryotes:

The relative abundance of the microbial communities (Figure 3) within all the samples (particulate trap material and seawater) were enriched by phyla belonging to *Proteobacteria* (29%), *Bacteroidetes* (12%), and *Cyanobacteria* (26%). The two dominant proteobacterial classes in the sequence libraries, *Alphaproteobacteria* and

Gammaproteobacteria, presented different environmental preferences that have been observed previously in the Sargasso Sea using qPCR 16S rRNA gene quantifications (Sjöstedt et al., 2014). In this study, the relative abundance of *Alphaproteobacteria* comprised 29% of the sequences and were mostly found as part of the spring prokaryotic community, with 11% relative abundance in particulate trap material and 32% in ambient seawater. In contrast, *Alphaproteobacteria* in the summer trap material had a higher relative abundance (7%) than the ambient seawater (4%). *Gammaproteobacteria* made up 18% of all the samples and were largely comprised of *Alteromonas sp.* (6%) and *Oleibacter sp.* (4%). *Alteromonas sp.* had a relatively low abundance of $\leq 1\%$ in samples from both seasons, except those from the summer trap material, where it contributed 30% to the sequence libraries. *Oleibacter sp.* had a similar trend, contributing generally $<1\%$ of the relative abundance, except those from the summer trap material (20%). Bacteroidetes (12%) were more abundant in the trap material (spring: 27%; summer: 13%) than in the seawater (spring: 11%; summer: 1%). The second most abundant class relative to the euphotic zone and shallow traps were the *Cyanobacteria* (26%), dominated by *Synechococcus* (12%) and *Prochlorococcus* (13%) and to a lesser extent, *Cyanobium* (3%). *Synechococcus* had a higher relative abundance in spring (seawater: 26%; trap material: 26%) than in the summer libraries (seawater: 0.1%; trap material: 1%). A similar trend was followed by *Prochlorococcus*, having more relative abundance in spring (seawater: 7%; trap material: 4%) and less in the summer (seawater: 3%; trap material: 2%). *Cyanobium* also contributed more to the spring (seawater: 1%; trap:2%) than the summer (seawater: 0.2% trap: 0.02%).

The non-metric multidimensional scaling ordination based on Bray-Curtis dissimilarities (stress = 0.119; Figure 4) revealed a compositional difference between the seawater and particulate trap material communities. After assessing the community differences within each sample type (Table 3), I found that only season ($R^2 = 0.228$; FDR = 0.009) and depth ($R^2 = 0.258$; FDR = 0.003) were significant predictors for prokaryotic communities in the euphotic zone, while no significant predictor for variability was found in the particulate trap material across all samples. Furthermore, after assessing intra-seasonal variations for the euphotic zone, only depth explained variation ($R^2 = 0.491$; FDR = 0.030) in the summer, but not in the spring, and no other predictors were found to significantly influence intra-seasonal variability.

The UPGMA dendrogram confirmed the clustering based on season, depth, and sample type. The prokaryotic communities of all trap samples clustered together, except for that of the community of a sample taken in cyclonic eddy C2, which clustered by season and location with the seawater communities, while seawater samples clustered by depth and season. No samples presented significant compositional differences (SIMPROF, $p < 0.05$; Figure 3) within each cluster, except the other C2 trap material sample, which was significantly different from the summer PITs.

Alpha diversity metrics among the prokaryotes, calculated as observed features (Figure 5a) and assessed with the Kruskal-Wallis H test ($H(5) = 19.7$, $P = 0.001$), were significantly different. The *post hoc* pairwise comparisons showed significant differences between the deep-chlorophyll maximum and the particulate trap material in spring ($P_{FDR-corrected} = 0.04$) and summer ($P_{FDR-corrected} = 0.007$). At the same time, the richness within the 20m depth community from both seasons was not significantly different from each

other and the other depths (DCM and PITs) of both seasons. The DCM community sampled in both seasons had the highest richness (spring $\hat{\mu}_{median} = 548.5$, summer $\hat{\mu}_{median} = 578$) compared to the rest of the samples. After applying a pairwise comparison of the species diversity calculated as Shannon's index (Figure 5b), and assessed with the Kruskal-Wallis H test ($H(5) = 17.25$, $P = 0.004$), I found that in spring, the communities at 20 m depth were significantly different ($P_{FDR-corrected} = 0.05$) from the communities of the DCM of the same season. Still, the DCM community was not different from the trap material. Conversely, I found that the summer communities at 20 m depth were not significantly different from the DCM communities. However, the DCM summer community was significantly different ($P_{FDR-corrected} = 0.02$) from the communities on the sinking particles from the same season. Both seasons' prokaryotic communities from the DCM had the highest diversity indices (spring $\hat{\mu}_{median} = 7.44$, summer $\hat{\mu}_{median} = 7.79$).

To determine the strength of associations ($\alpha = 0.05$) between the taxa and the a priori groups (seawater and sinking particles), I performed an Indicator Species Analysis (Figure 6). After correcting for multiple comparisons ($P_{FDR-corrected} < 0.05$, Benjamini-Hochberg) to identify the list of indicators in each sample type, I found 31 species to be indicators for the particle trap material and 14 species for the seawater in both seasons. Indicators for seawater were taxa predominantly within *Proteobacteria*, such as the alphaproteobacterial order *Rickettsiales*, the gammaproteobacterial order *Pseudomonadales*, and the alphaproteobacterial SAR 11 clade. In contrast, the indicator taxa for the trap samples were dominated by *Bacteroidota*, *Proteobacteria*, and to a lesser extent, *Verrucomicrobiota*. Three of the four indicator taxa in sinking particles with the highest indicator value possible were from the gammaproteobacterial order

Pseudomonadales, one of which was *Umboniibacter sp.*. In addition, proteobacterial taxa that have been previously linked to sinking particles (Cruz et al., 2021; Fontanez et al., 2015) were also present as indicator species, such as *Vibrio sp.*, *Pseudoalteromonas sp.*, and *Erythrobacter sp.* with high indicator values (≥ 0.8). Interestingly, the Indicator Species Analysis using the group combination of both sample types identified *Synechococcus*, *Prochlorococcus*, and *Cyanobium* as the only *Cyanobacteria* equally present in seawater and trap material within the same season and with the highest indicator value possible (i.e., during the same season, they are generalist taxa equally found within this set of samples; Table 5). However, because there is no other set of samples or reference dataset that does not contain these three cyanobacteria, I cannot calculate the *p-values* (De Cáceres, 2022).

To identify the taxa that drove the significant ($P_{FDR-corrected} < 0.05$) community difference between seawater and particle trap material in both seasons (Figure 7a–7b), I performed a differential abundance analysis. Taxa previously identified as indicators of the particle trap material in this study, such as *Reichenbachiella sp.*, *Photobacterium sp.*, *Lentisphaera sp.*, *Erythrobacter sp.* and *Vibrio sp.*, were also significantly differentially abundant in the trap material from the spring (Figure 7a). Indicators identified for seawater in this study also drove community differences in the spring samples, like *Rhodobacteraceae*, SAR11, and *Dadabacteriales*, while *Synechococcus sp.* and *Prochlorococcus sp.* were some of the taxa with the most significant \log_2 -fold change in the spring euphotic zone community. Indicator taxa for particle trap material were less present in the differential abundance analysis for summer (Figure 7b), but the ones present were *Vibrio sp.*, unknown *Rhodobacteraceae*, *Reichenbachiella sp.*, and *Lentisphaera sp.*

In this season, the taxon with the highest log₂-fold change value was *Halomonas* sp.. Notably, *Photobacterium* sp. and *Lenthisphaera* sp. were significantly more abundant in sinking particles during both seasons, while *Oleibacter* sp. was only present in the particles collected during summer. *Prochlorococcus* sp. and SAR11 primarily drove the differential abundance in seawater, while *Synechococcus* sp. was also differently abundant in the seawater during both seasons.

Photoautotrophs

The community of photoautotrophs (Figure 8) in all the samples (trap material and seawater) were mainly enriched by the phyla *Haptophyta* (8%), *Ochrophyta* (7%), and *Chlorophyta* (2%) relative to *Cyanobacteria* (30%). Within the *Haptophyta*, the *Prymnesiophyceae* were found with lower relative abundance in ambient seawater (spring: 13%; summer: 13%) but enriched in the trap material (spring: 36%; summer: 25%). The *Phaeocystales* order, *Prymnesiophyceae*, drove the composition for this class, with a smaller relative abundance in ambient seawater (spring: 8%; summer: 29%) compared to particulate trap material (spring: 22%; summer: 12%). Members of the mostly photosynthetic heterokont, *Ochrophyta*, were the second most abundant phylum of phototrophs in the library. However, the summer trap libraries had the highest abundance (36%), compared to spring (8%) and ambient seawater (spring: 8%; summer: 10%). Among the *Bacillariophyta*, *Rhizosolenia* sp. had major contributions in the summer trap libraries with 13% of the relative abundance but only < 1% in the water column of both seasons and the particle community in spring. *Chaetoceros* sp. and other unidentified members of the *Bacillariophyta* contributed to the summer trap material, totaling 36%, while contributing < 3% to the photosynthetic community in all other samples (i.e., seawater and

traps). The third most abundant phylum, *Chlorophyta*, had two members of the *Mamiellales* class, *Ostreococcus* sp. and *Bathycoccus* sp., that contributed to the higher abundance of chlorophytes in the spring water column (7%). In contrast, the members of the novel *Chloropicophyceae* class, *Chloroparvula* sp. and *Chloropicon* sp., contributed to the higher abundance of chlorophytes in the summer water column (3%). Additionally, the trap material for both seasons was enriched in *Chloropicales* (spring: 5%; summer: 2%) compared to the *Mamiellales*, which had <1% in the trap material from both seasons. The most abundant class was the *Cyanobacteria* (30%), in which *Prochlorococcus* sp. (16%) and *Synechococcus* sp. (12%) dominated. *Prochlorococcus* sp. was less abundant in the spring (seawater: 17%, trap material: 5%) and more abundant in the summer (seawater: 62%, trap material: 7%) but consistently overrepresented in the seawater. The inverse trend was exhibited by *Synechococcus* sp., being abundantly present in the spring (seawater: 50%, trap material: 32%) and less abundant in the summer (seawater: 7%, trap material: 4%).

The NMDS based on Bray-Curtis dissimilarities (stress = 0.122; Figure 9) revealed overlapping ellipses (CI = 95%) that appear to have a weak visual separation by depth between seawater and particulate trap material; however, influenced by the seasonal separation of all samples. After assessing the variability with PERMANOVA, I found that season ($R^2 = 0.245$, $P_{FDR-corrected} = 0.005$), depth ($R^2 = 0.349$, $P_{FDR-corrected} = 0.005$), sample type ($R^2 = 0.171$, $P_{FDR-corrected} = 0.01$), and eddy location ($R^2 = 0.350$, $P_{FDR-corrected} = 0.009$) were significant predictors. The UPGMA dendrogram of the photoautotrophs also confirmed clustering based on season, depth, and sample type. Interestingly, the libraries of two spring samples, C2 PITs and DCM BATS, were part of a spring water column

cluster, although the two were significantly different (SIMPROF, $p < 0.05$; Figure 8). Similarly, one Ace2 DCM sample clustered with the spring 20 m depth, although significantly different from those samples. Finally, the other C2 PITs were significantly different from the other particulate trap samples libraries, even though it clustered with those samples.

When assessing the richness (observed features) among the photoautotrophic eukaryotes (Figure 10a) relative to *Cyanobacteria* ($H(5) = 8.48$, $P = 0.13$), I found that none of the groups were significantly different from each other as determined by the Dunn's test pairwise comparison. After comparing the diversity (Figure 10b) within all samples (Shannon's index, $H(5) = 16.09$, $P = 0.007$), I found that the summer 20 m depth community had the lowest index ($\hat{\mu}_{median} = 2.83$) and was significantly different from the DCM ($P_{FDR-corrected} = 0.04$) and PITs ($P_{FDR-corrected} = 0.04$) communities of the same season. The 20 m depth community in spring was also significantly different from the summer particle community ($P_{FDR-corrected} = 0.04$).

In the indicator species analysis of the photoautotrophic community (Figure 11), I only found one taxon, the nano-sized heterokont, *Florenciella parvula* (*Dictyochophyceae*), with a high indicator value (≥ 0.8) in the seawater, but it was not significant ($\alpha < 0.05$, $P_{FDR-corrected} = 0.2$). However, I found four taxa to be indicators of particle libraries: the cryptophyte *Teleaulax sp.*, the diatom *Chaetoceros sp.*, and two members of pico-prasinophytes, *Chloropicon sp.* and *Chloroparvula sp.*, a genus within the relatively novel class *Chloropicophyceae* (Lopes Dos Santos et al., 2017). Moreover, *Rhizosolenia sp.* was identified as an indicator of the summer particles, but not for the spring trap libraries, agreeing with their relative abundance contribution discussed above.

The generalist taxa identified to have the highest value possible for fidelity and specificity to all *a priori* groups were four members of prymnesiophytes, which included *Emiliana* sp. and *Phaeocystis* sp., and two unknown ASVs within the class *Prymnesiophyceae*. I also found the two picocyanobacteria, *Synechococcus* sp. and *Prochlorococcus* sp., to be indicators of generalist taxa in all samples.

Within the spring euphotic zone community, *Synechococcus* sp. was the taxon with the highest log₂-fold change value and abundance (Figure 12a), followed by *Bathycoccus* sp. and the cryptophyte order *Cryptomonadales*. Only the cryptophyte *Teleaulax* sp. was differently abundant in trap libraries in spring, which confirms this genus as indicator taxon identified in this study. In summer, *Prochlorococcus* sp. had the highest log₂-fold change and mean abundance in the water column (Figure 12b), followed by the pico-prasinophyte, *Ostreococcus* sp., and the picocyanobacterial species, *Synechococcus*. Lastly, the differential abundance analysis revealed that the centric diatom, *Rhizosolenia* sp., was significant ($P_{FDR-corrected} < 0.05$) for the summer particle community, having the highest mean abundance and log₂-fold change, though it only appeared in the center of the anticyclonic eddy (AC2). The other taxa that were both overrepresented in the traps in summer, ($P_{FDR-corrected} < 0.05$) and identified as indicator taxa were the diatom *Chaetoceros* sp. and the cryptophyte *Teleaulax* sp., with the addition of an unknown bacterial ASV in the plastidial library.

DISCUSSION

The understanding of microbial abundance and its dynamics in the ocean has been rapidly evolving thanks to the revolution in sequencing technology during the past few

years (Pedrós-Alió, 2012). This has helped better understand the regimes in which rare and dominant communities are modified and structured throughout the ocean biosphere. For example, in nutrient-poor conditions, such as those found in the Sargasso Sea, slow-growing oligotrophic microorganisms generally dominate the water column and exhibit high surface-to-volume ratios and small genome sizes that promote phylogenetic hierarchy and partitioning (Giovannoni et al., 2014). On the other hand, the nutrient-rich patches found throughout these ocean "deserts", like particulate organic matter, harbor microbial "hotspots" for fast-growing copiotrophic microorganisms (Fontanez et al., 2015). Therefore, while only a few taxa dominate the abundance and distribution of microbial communities, less abundant taxa constitute most of the microbial diversity. Moreover, marine pelagic ecosystems present bottom-up and top-down controls of community structure through the availability of nutrients and grazing pressures, respectively (Troussellier et al., 2017). These and other environmental variations (e.g., season) and stochastic events are important drivers of microbial diversity (Lynch & Neufeld, 2015; Troussellier et al., 2017). Therefore, through this study, I shed light on the potential connections between the microbial communities in the euphotic zone and those in sinking particles collected with shallow traps in the Sargasso Sea using high-throughput sequencing of 16S rDNA. I assessed the microbial communities by using a degenerate universal primer set (515Y/926R) that enabled the taxonomic identification of prokaryotes and eukaryotic phototrophs through their plastidial DNA (Parada et al., 2016). Although large phytoplankton can have variations in the 16S rRNA gene copy numbers because of their high number of chloroplasts (dozens to hundreds) compared to small phytoplankton (1-2 copies per cell), it is much less compared to the 18S gene copy numbers that can range

from 10 to ca. 50,000 copies per cell (Needham & Fuhrman, 2016). Yeh and colleagues (2021) assessed the primer bias with 16S and 18S mock communities, and proposed that using the chloroplast 16S genes amplified with 515Y/926R more closely reflects phytoplankton biomass distribution. With this approach, I show the co-occurrence of picophytoplankton and larger-sized phytoplankton, and hypothesize that episodic events such as eddy/wind interactions resulted in higher export of POC. Moreover, I identify a catalog of microbial taxa that are specifically and constantly found in sinking particles within this study by conducting an Indicator Species Analysis. I also discern the microbial communities that are differently abundant in the euphotic zone and sinking particles. Lastly, I show the importance of studying the influence of physical forcing on the microbial community variability in the Sargasso Sea.

Community structure as evidence of complex microbial interactions

The seasonal differences in the prokaryotic community structure between the euphotic zone and shallow trap samples were mainly driven by the taxa of *Proteobacteria*, *Bacteroidia*, and *Cyanobacteria* (Figure 3). In contrast to the well-studied seasonal contribution of *Prochlorococcus* and *Synechococcus* (Parsons et al., 2012), I found that the relative abundance of both cyanobacteria was higher in the spring. However, the highest number of 16S rDNA sequences of the same libraries recovered from *Prochlorococcus* was found in the summer euphotic zone (14,733), compared to the spring (3,519). Field observation of the same cruises using clade-specific qPCR primers determined that *Prochlorococcus* was more abundant in the summer (De Martini et al., 2018). Therefore, the compositional nature of microbiome datasets needs to be taken into consideration as

this influences the relative distribution of the taxa found within the samples (Gloor et al., 2017). Moreover, I was able to resolve the well-studied seasonal distribution of *Prochlorococcus* (De Martini et al., 2018) using the PR² database, which includes PhytoREF. I posit that using this database is helpful for deciphering the dynamics of *Cyanobacteria* when used in conjunction with plastidial rDNA sequences.

The oligotrophic alphaproteobacteria were enriched in the water column, specifically with the ubiquitous and abundant SAR11 (Giovannoni, 2017). This chemoheterotroph dominated the water column in spring (Figure 7a). Nevertheless, it also drove part of the community difference during the summer, as determined by the differential abundance analysis (Figure 7b) where it co-occurred with *Prochlorococcus*. This co-occurrence could arise from the dependency that SAR11 has evolved, utilizing glycolate and pyruvate from *Prochlorococcus* (Braakman et al., 2017). Morris and colleagues (2012) proposed the *Black Queen Hypothesis* to explain the co-dependency of *Prochlorococcus* and SAR11. Both oligotrophic microbes have reduced metabolic and genomic functions that limit the amount of carbon and nutrients required to sustain life (Giovannoni et al., 2014). For example, SAR11 has evolved to metabolize dissolved organic carbon of low molecular weight and, therefore, utilizes the leaky products that usually occur in phytoplankton assemblages (Becker et al., 2019; Giovannoni, 2017; Giovannoni et al., 2014).

The differential abundance analysis comparing the microbial communities in the euphotic zone revealed a large catalog of microbial lineages overrepresented in the spring (Figure 7a) compared to the summer (Figure 7b). This may suggest that pelagic microbes during the early spring sampling were experiencing less bottom-up controls that promoted

their diversity in the water column. While the passing of mesoscale features may induce upwelling, decaying features such as was suggested for the cyclone C2 (Cotti-Rausch et al., 2016), generally do not induce a biological response (Sweeney et al., 2003). Other factors that may play a role in the higher diversity of microbial lineages in the water column in spring (Figure 5a) are the diverse metabolic life styles that are necessary for life in nutrient-poor environments (García-Martín et al., 2019).

De Martini and colleagues (2018) documented the distribution of *Prochlorococcus* for the same cruises by applying clade-specific qPCR primers. They found the MIT 9313 low-light adapted (LL) strain only at depths below 80 m during the summer. In phosphorus-limited conditions, such as those found in the Sargasso Sea (Cianca et al., 2007; Helmke et al., 2010), cells can excrete significantly less carbon that consists of dead-end carbon products such as small carboxylic acids like glycolate and pyruvate (Bertilsson et al., 2005; Braaksman et al., 2017). The high-light (HL) adapted strains of *Prochlorococcus* are not able to utilize their metabolites as a carbon source; however, the MIT 9313 low-light IV (LLIV) clade has the genomic machinery for recycling their own glycolate through the iron-sulfur protein glycolate oxidase, efficiently utilizing dissolved organic carbon during environmental stress. This gain in function and ecotype partitioning can be explained by the higher number of sigma factors that LL strains possess compared to their HL counterparts (Scanlan et al., 2009).

While pyruvate secretion can serve as a peroxide scavenger in the absence of catalases (Kim et al., 2021), neither SAR11 nor *Prochlorococcus* have the genes to detoxify the ubiquitously abundant hydrogen peroxide, a strong oxidant. Therefore, they rely on catalase-positive heterotrophic bacteria. For example, co-culture experiments of

Prochlorococcus using the gammaproteobacterial genus *Alteromonas* and *Vibrio* with insertional inactivation of catalase activity led to a loss of growth in the cultured picocyanobacteria, while the presence of catalase activity had the opposite results (Morris et al., 2011). It is noteworthy that the sphingobacteria, *Marinimicrobia* (SAR406) in the samples, while low in relative abundance, were enriched at 100 m depth during the summer. SAR406 are heme auxotrophic *Bacteroidetes*; therefore, they rely on the catalases of peroxide-degrading microbes to thrive (Kim et al., 2021) and are tied to nitrate reduction, dissimilatory nitrate reduction to ammonia, and sulfur reduction (Thrash et al., 2017), processes that suggest metabolic cooperation (Hawley et al., 2017). *Synechococcus*, a close-relative of *Prochlorococcus*, has been shown to have weak catalase activity (Morris et al., 2011) and therefore benefit from helper bacteria that break down catalase (Morris et al., 2008; Zinser, 2018). However, *Synechococcus* has the gene *thiC* that encodes for the complete biosynthesis of vitamin B₁ at nanomolar concentrations. Gene profiles of *thiC* in the Sargasso Sea during September 2012 revealed that its expression increases with depths below 80 m, and it is exacerbated in the deep chlorophyll maximum (Carini et al., 2014). The release of vitamin B₁ benefits pelagic bacteria like SAR11, that lack a complete thiamin biosynthetic pathway. While disentangling metabolic pathways is out of the scope of this work, understanding the plausible metabolic cooperation between pelagic bacteria may help understand their abundance and distribution throughout the euphotic zone.

The communities of the sinking particles collected for this study were overrepresented by the copiotrophic class, *Gammaproteobacteria*, consistent with other studies (Boeuf et al., 2019; Cruz et al., 2021; Fontanez et al., 2015). However, the mechanisms that lead to their enrichment in the marine particles may vary. For example,

Raina et al. (2022) used *in situ* chemotaxis assays and found that members of *Pseudoalteromonas* and *Vibrio* were generalist, motile taxa significantly enriched in most of the phytoplankton-derived dissolved organic matter they studied, including those produced by *Synechococcus* and the diatom *Chaetoceros*. This motility increases particle encounter rates on the scale of minutes to hours (Lambert et al., 2019), therefore is an important behavior in the patchy nutrient environments of the oligotrophic Sargasso Sea.

The indicator species analysis (Figure 6) also revealed a catalog of important copiotrophic microbes commonly known to colonize particles, like *Pseudoalteromonas* sp. and *Vibrio* sp (Cruz et al., 2021; Fontanez et al., 2015). Interestingly, the taxon with the highest indicator value was *Umboniibacter*, a species isolated from tissues of marine mollusks (Romanenko et al., 2010), also reported as an indicator by Cruz et al. (2021); however, it was one of the less abundant indicator taxa within this study. Furthermore, *Oleibacter* sp., *Alteromonas* sp., and other important hydrocarbonclastic microbes were significantly differentially abundant in the spring particle traps relative to the seawater (Figure 7a). The presence of *Oleibacter* sp. in marine particles has been previously found in oligotrophic regions of the equatorial Pacific (Guevara Campoverde et al., 2018), where *Chaetoceros* sp., *Emiliana* sp., and *Thalassiosira* sp. were presumably the dominant primary producers. According to the indicator analysis of photoautotrophs (this will be discussed in detail in the next section), *Emiliana* sp. was a generalist phytoplankton found in the euphotic zone and marine particles of both seasons (Table 6). In contrast, *Thalassiosira* sp. was only found to be an indicator for the summer particle trap libraries, and *Chaetoceros* sp. was an indicator of sinking particle communities in both seasons

(Figure 12). However, if the presence of *Oleibacter* sp. in the spring particles was connected to exudates from *Chaetoceros* sp. and/or *Emiliana* sp., remains unclear.

Furthermore, the indicator and differential abundance analysis (Figures 6–7) revealed that *Photobacterium* sp. and *Tenacibaculum* sp. were important contributors to marine particle libraries in both seasons. *Photobacterium* is a generalist chemotactic bacterium (Raina et al., 2022) involved in nitrogen cycling (Bik et al., 2019), and *Tenacibaculum* sp. is an important marine fish pathogen (Piñeiro-Vidal et al., 2008) usually categorized as surface-associated microbe (Frette et al., 2004). Mestre and colleagues (2017) did a particle study using size-fractions from 0.2 to 200 μm (pico- and microplankton sizes, respectively) collected in the oligotrophic coastal region of the Mediterranean Sea. According to the authors, this region is usually dominated by prymnesiophytes and episodically, *Bacillariophyta*. They found that the flavobacteria, *Tenacibaculum* sp., was an indicator of their larger particulate size fractions, but they did not indicate which size. Moreover, Raina et al. (2022) found in their chemotaxis assay that flavobacteria present more specialized relationships with the phytoplankton they colonize than *Gammaproteobacteria*.

According to the indicator taxa analysis, the relative abundance of both *Photobacterium* sp. and *Tenacibaculum* sp. in the particles collected at the edge of the anticyclonic eddy paled in comparison to the much greater relative abundance in the particle libraries of the other stations from both seasons. This scenario was repeated with the rest of the indicator taxa identified in the trap samples, except *Pseudoalteromonas* sp. which presented a high abundance in particles of all stations. Mestre et al. (2017) found that the microbial community of the larger size-fraction are generally more diverse but less

abundant than those of the smaller size-fractions. The lower diversity within smaller size-fractions (0.2–3.0 μm) is not surprising, as this range generally captures the free-living portion of planktonic microorganisms. However, their finding that more specialized but less abundant microbes are found as the particle size increases is interesting. While my study does not elucidate the different sinking particle size fractions that can be captured with the surface tethered traps, by studying the microbial diversity, I can entertain ideas of what type of particle size dominated the sinking particles during the time of the sampling.

As mentioned previously, *Gammaproteobacteria* were overrepresented in the marine particles. While seasonal transition to warmer temperatures (i.e., spring and summer) can increase the motility of copiotrophs (Grossart et al., 2001), biological pressures like viral lysis (Parsons et al., 2012) and bacterivory (Gong et al. 2016) play important roles in the distribution of marine microbes. It has also been shown that alpha- and gammaproteobacteria can present resistance to digestion from ciliated protozoa (Gong et al., 2016). This may offer an opportunity for copiotrophs to be incorporated as undigested cells into sinking particles, similar to *Synechococcus* (Richardson & Jackson, 2007; Schnetzer & Steinberg, 2002; Wilson & Steinberg, 2010). The trap samples also revealed the presence of other widely diverse and ecologically important *Bacteroidetes*, mainly within the orders of *Flavobacteriales* and *Cytophagales*. *Bacteroidetes*, in general, are known to hydrolyze polysaccharides, and *Cytophagales* are primarily composed of heterotrophic motile bacteria. *Bacteroidetes* have also been found to colonize marine particles (Woebken et al., 2007) and transparent exopolymeric particles (Pedrotti et al., 2009).

Photoautotrophic community of large diatom dominates particle export

The abundance of the photoautotrophic plankton as determined by sequence libraries of plastidial 16S rDNA in the euphotic zone showed a seasonal pattern driven by picocyanobacteria, which in turn influenced their occurrence within the trap sample libraries. *Prochlorococcus* was proportionally overrepresented in the summer euphotic zone libraries compared to the trap libraries of the same season. Their high relative abundance in the upper euphotic zone to the deep-chlorophyll maximum indicates the well-known adaptation to different light regimes (Rocap et al., 2002). I also identified contributions from *Prochlorococcus* sp. to the summer trap samples collected at the edge of the anticyclonic eddy (Figure 8). Nevertheless, their contribution paled in comparison to those of the prymnesiophyte, *Phaeocystis* sp., and the large centric diatom *Rhizosolenia* sp. in particles collected at the center of the same eddy. Culture-based studies on the grazing pressure upon *Phaeocystis* have demonstrated a trophic linkage between *Phaeocystis*, dinoflagellates, and phagotrophic protists (Tang et al., 2001). The authors explain that the polyunsaturated fatty acids of *Phaeocystis globosa* are of low nutritional value relative to other available prey (e.g., *Rhodomonas salina*), which reduces their grazing pressure; however, ciliates can still prey on intermediate grazers like heterotrophic dinoflagellates. The copepod predation on ciliates further relaxes grazing pressure on *Phaeocystis* sp., therefore, promoting bloom events (Hansen et al., 1994; Tang et al., 2001). *Phaeocystis* sp. can also produce sticky transparent exopolymeric particles that promote aggregation (Passow & Wassmann, 1994). Mesocosm studies with nutrient poor water demonstrated that *Phaeocystis* sp. exudes two types of TEP depending on the limiting nutrient (Mari et al., 2005). Furthermore, when they were found in N-limited conditions,

Phaeocystis aggregated less than when found in a P-limited environment. The depletion of phosphorus promoted a massive release of heavy mucous aggregates, suggesting a larger contribution to carbon export in this condition (Mari et al., 2005). This adaptation is important as enzyme linked fluorescent assays (Lomas et al., 2004) and measurements of the P-specific enzyme alkaline phosphatase (Mather et al., 2008) have suggested the Sargasso Sea to be limited in inorganic phosphorus.

Pigment analyses to determine phytoplankton composition and biomass were reported from the same stations by Cotti-Raush and colleagues (2016), and they generally found little diatom presence in the euphotic zone during both seasons, but with some contribution in the DCM of the anticyclonic eddy AC2. The DNA analysis done for this study confirms this distribution. However, the presence of the large diatom *Rhizosolenia* in the particle traps deployed in the center of the warm-core eddy, while being nearly absent in the euphotic zone (only 14 sequences found in the deep chlorophyll maximum) is of interest as it suggests the sedimentation of a bloom event that happened before the arrival at the site. The significance of the contribution of *Rhizosolenia* to the summer particle trap community is confirmed by the differential abundance analysis of the summer traps relative to the euphotic zone (Figure 12b). It is noteworthy that *Rhizosolenia* mats are known for vertically migrating below the euphotic zone in the central North Pacific to exploit nitrogen pools (Villareal et al., 1996), therefore efficient at growing in low-light intensities. This may explain why sampling efforts did not capture this centric diatom community. Batch-culture studies of *Stephanopyxis palmeriana*, although not found in this study, provided another example of a diatom that, while adapted to growing at low light intensities, could potentially meet new production estimates sufficient to offset geochemical imbalances in

the Sargasso Sea (Goldman & McGillicuddy, 2003). Furthermore, Goldman and colleagues (1993; 2003) demonstrated that annual new production in the Sargasso Sea could be attributed to upwelling events caused by mesoscale eddies that promote the growth of large diatoms residing at the base of the euphotic zone. While anticyclones are not characterized by upwelling in their center, the eddy/wind interactions found for this eddy (Cotti-Rausch et al., 2016, DeMartini et al., 2018) and the increased particle flux at the eddy center (21.9 POC mg C m⁻² d⁻¹) compared to the eddy edge (7.9 POC mg C m⁻² d⁻¹), and BATS (5.3 POC mg C m⁻² d⁻¹) points to the export of a large diatom community by an episodic upwelling eddy event.

Another evidence for an upwelling event during the anticyclonic eddy is the presence of pelagophytes, specifically, *Pelagomonas sp.* The pigment analysis related to this study found the presence of pelagophytes at the DCM of the summer euphotic zone (Cotti-Rausch et al., 2016), which is in accordance with my findings. This picoplanktonic pelagophyte can be efficient at nitrogen assimilation by activating depth-specific genes of bacteria-like systems for nitrogen sensing (Dupont et al., 2015). Their presence at the deep chlorophyll maximum and within the shallow traps suggests that they significantly contribute to new production, as *Pelagomonas* has been found to dominate nitrate uptake in nutrient-poor conditions (Guérin et al., 2021). Worden et al. (2012) used fluorescence-activated cell sorting (FACS) in tandem with targeted metagenomics and assembled the complete genome of *Pelagomonas*. They then studied the global distribution of pelagophytes to compare with the assembled chloroplast genome and highlighted the importance of this picophytoplankton group to carbon flux in the North Pacific because of their presence in deep-sea sediments.

In this study, I also show that prasinophytes within the *Prasinococcales* order were more dominant in the particle traps of the anticyclonic eddy center than throughout the euphotic zone during both seasons. Pigment analysis of prasinophytes indicates that they were mostly present at depths at or below the deep chlorophyll maximum (Cotti-Rausch et al., 2016). The indicator species analysis agrees with those findings, as *Prasinococcales* were identified as indicators of the particle traps and summer euphotic zone. Furthermore, pigment analysis in the northern Sargasso Sea revealed the combination of prasinophytes, pelagophytes, diatoms, and dinoflagellates during mode water eddies (Ewart et al., 2008). Although *Prasinococcales* sequences were not resolved to genus level, I can make assumptions that pico-prasinophytes were abundantly present in particle traps as *Prasinoderma* and *Prasinococcus* are the only genera within the *Prasinococcales* order (Guiry and Guiry, 2012). In addition, picophytoplankton of the Mamiellales order, *Bathycoccus*, and *Ostreococcus* were mainly enriched in the DCM at BATS during both seasons, outside of the mesoscale features with the exception of one DCM sample from cyclone C2. Indicator species analysis confirms this distribution as *Bathycoccus* and *Ostreococcus* are classified as indicators for the euphotic zone during both seasons, although not significantly (Table 6). Moreover, the differential abundance analysis further agrees with these findings as it revealed that *Bathycoccus* was differently abundant in the spring euphotic zone (Figure 12a) and *Ostreococcus* in the summer euphotic zone (Figure 12b). In contrast to these results, Bianca et al. (2021) found *Bathycoccus* to be an indicator of phytodetrital and fecal pellet aggregates collected in the Sargasso Sea, while picocyanobacteria contributed ca. 2% or less to the microbial community in the particles and seawater during their fall 2017 and spring 2018 cruises. Similarly, Treusch et al. (2012)

used qPCR to quantify the distribution of the pico-prasinophytes in the Sargasso Sea and found that *Bathycoccus* and *Ostreococcus* are generally more abundant during a period in which picocyanobacteria have the lowest contributions to 16S rRNA gene signals and when dilution of grazing pressure occurs due to deep mixing events. In contrast to the pico-prasinophytes *Ostreococcus* and *Bathycoccus*, the relatively novel pico-prasinophytes, *Chloropicon* and *Chloroparvula*, significantly contributed to the particle communities as identified by the indicator species analysis. Bolaños et al. (2020) found picocyanobacteria, pico-prasinophytes, and nanophytoplankton were major contributors to planktonic assemblages when large diatoms and other larger phytoplankton were generally infrequent. Lastly, both the indicator species analysis and differential abundance analysis found the significant contribution of *Chaetoceros* and *Teleaulax* to the marine particles collected for this study. Culture studies and genotyping of natural assemblages done by Tanković et al. (2018) show that *Chaetoceros* increase their effective cell size when found in P-limited conditions. Moreover, they found that *Chaetoceros* are opportunistic diatoms that grow when nutrient and phytoplankton abundances are lower. While they were identified as indicator taxa of the particle traps, their contribution to abundance was generally low compared to other phytoplankton and negligible in the euphotic zone during both seasons. Together, these results suggest that small phytoplankton are important contributors to carbon export. At the same time, an episodic eddy upwelling in stratified waters increased the contribution of larger phytoplankton in the oligotrophic Sargasso Sea in the summer of 2012.

Contribution of picophytoplankton to particle flux

The size fractions of pico- (0.7–2 μm), nano- (2–20 μm), and microphytoplankton- (20–200 μm) indicated that picophytoplankton explained 84% of the total integrated chlorophyll- α variability and 87% of the PP variability with depth (Cotti-Rausch et al., 2020). However, no correlations between the two variables were found. During the cruises, picophytoplankton contributed the most to both biomass and primary production (Cotti-Rausch et al., 2020). At the same time, the highest primary productivity during the cruises was found in the upper 50 m (4 mg C m³ d⁻¹). The lowest was at 100 m (< 1 mg C m³ d⁻¹), but this variability was always driven by picophytoplankton, not by larger phytoplankton. In addition, the three-decade time series analysis of the BATS site points to an adapted carbon export in the 2010s (Lomas et al., 2022). During this decade, larger phytoplankton presented year-long low abundances compared to previous decades, while warmer temperatures and lower nutrient inventories characterized the euphotic zone. In contrast, picocyanobacterial abundances were higher with depth, having peaks at the base of the euphotic zone (~100 m) due to the vicinity of the nutricline. Despite unfavorable conditions for carbon export mediated by larger phytoplankton, the export efficiency was not affected. I conclude that episodic eddy upwelling events that lead to a rapid increase of larger and opportunistic phytoplankton make an important contribution to new production. The significant contribution of *Rhizosolenia* to the particle community of the anticyclone center that experienced upwelling further confirms the importance of physical forcing mechanisms on the biological community. These processes in seasonally stratified regions such as the Sargasso Sea (Helmke et al., 2010) are of special importance as oligotrophic regions are thought to expand on a future warmer planet (Polovina et al., 2008).

REFERENCES

- Amacher, J., Neuer, S., Anderson, I., & Massana, R. (2009). Molecular approach to determine contributions of the protist community to particle flux. *Deep-Sea Research Part I: Oceanographic Research Papers*, 56(12), 2206–2215. <https://doi.org/10.1016/j.dsr.2009.08.007>
- Amacher, J., Neuer, S., & Lomas, M. (2013). DNA-based molecular fingerprinting of eukaryotic protists and cyanobacteria contributing to sinking particle flux at the Bermuda Atlantic time-series study. *Deep-Sea Research Part II: Topical Studies in Oceanography*, 93, 71–83. <https://doi.org/10.1016/j.dsr2.2013.01.001>
- Andersen, N. G., Nielsen, T. G., Jakobsen, H. H., Munk, P., & Riemann, L. (2011). Distribution and production of plankton communities in the subtropical convergence zone of the Sargasso Sea. II. Protozooplankton and copepods. *Marine Ecology Progress Series*, 426(March), 71–86. <https://doi.org/10.3354/meps09047>
- Anderson, M. J. (2001). A new method for non-parametric multivariate analysis of variance. *Austral Ecology*, 26(1), 32–46. <https://doi.org/10.1046/j.1442-9993.2001.01070.x>
- Baumas, C. M. J., Le Moigne, F. A. C., Garel, M., Bhairy, N., Guasco, S., Riou, V., Armougom, F., Grossart, H. P., & Tamburini, C. (2021). Mesopelagic microbial carbon production correlates with diversity across different marine particle fractions. *ISME Journal*, 15(6), 1695–1708. <https://doi.org/10.1038/s41396-020-00880-z>
- Becker, J. W., Hogle, S. L., Rosendo, K., & Chisholm, S. W. (2019). Co-culture and biogeography of *Prochlorococcus* and SAR11. *ISME Journal*, 13(6), 1506–1519. <https://doi.org/10.1038/s41396-019-0365-4>
- Benjamini, Y., & Hochberg, Y. (1995). Controlling the False Discovery Rate: A Practical and Powerful Approach to Multiple Testing. *Journal of the Royal Statistical Society: Series B (Methodological)*, 57(1), 289–300. <https://doi.org/10.1111/j.2517-6161.1995.tb02031.x>
- Bertilsson, S., Berglund, O., Pullin, M. J., Chisholm, S. W. (2005). Release of dissolved organic matter by *Prochlorococcus*. *VIE ET MILIEU*, 55(3-4), 225–231
- Bibby, T. S., Gorbunov, M. Y., Wyman, K. W., & Falkowski, P. G. (2008). Photosynthetic community responses to upwelling in mesoscale eddies in the subtropical North Atlantic and Pacific Oceans. *Deep-Sea Research Part II: Topical Studies in Oceanography*, 55(10–13), 1310–1320. <https://doi.org/10.1016/j.dsr2.2008.01.014>
- Bik, H. M., Alexiev, A., Aulakh, S. K., Bharadwaj, L., Flanagan, J., Haggerty, J. M., Hird, S. M., Jospin, G., Lang, J. M., Sauder, L. A., Neufeld, J. D., Shaver, A., Sethi, A., Eisen, J. A., & Coil, D. A. (2019). Microbial Community Succession and Nutrient Cycling Responses following Perturbations of Experimental Saltwater

Aquaria. *MSphere*, 4(1). <https://doi.org/10.1128/msphere.00043-19>

- Boeuf, D., Edwards, B. R., Eppley, J. M., Hu, S. K., Poff, K. E., Romano, A. E., Caron, D. A., Karl, D. M., & DeLong, E. F. (2019). Biological composition and microbial dynamics of sinking particulate organic matter at abyssal depths in the oligotrophic open ocean. *Proceedings of the National Academy of Sciences of the United States of America*, 116(24), 11824–11832. <https://doi.org/10.1073/pnas.1903080116>
- Bolaños, L. M., Karp-Boss, L., Choi, C. J., Worden, A. Z., Graff, J. R., Haëntjens, N., Chase, A. P., Della Penna, A., Gaube, P., Morison, F., Menden-Deuer, S., Westberry, T. K., O'Malley, R. T., Boss, E., Behrenfeld, M. J., & Giovannoni, S. J. (2020). Small phytoplankton dominate western North Atlantic biomass. *ISME Journal*, 14(7), 1663–1674. <https://doi.org/10.1038/s41396-020-0636-0>
- Boyd, P. W., Claustre, H., Levy, M., Siegel, D. A., & Weber, T. (2019). Multi-faceted particle pumps drive carbon sequestration in the ocean. *Nature*, 568(7752), 327–335. <https://doi.org/10.1038/s41586-019-1098-2>
- Braakman, R., Follows, M. J., & Chisholm, S. W. (2017). Metabolic evolution and the self-organization of ecosystems. *Proceedings of the National Academy of Sciences of the United States of America*, 114(15), E3091–E3100. <https://doi.org/10.1073/pnas.1619573114>
- Buesseler, K. O., Antia, A. N., Chen, M., Fowler, S. W., Gardner, W. D., Gustafsson, O., Harada, K., Michaels, A. F., van der Loeff, M. R., Sarin, M., Steinberg, D. K., & Trull, T. (2007). An assessment of the use of sediment traps for estimating upper ocean particle fluxes. *Journal of Marine Research*, 65(3), 345–416. <https://doi.org/10.1357/002224007781567621>
- Buesseler, K. O., Boyd, P. W., Black, E. E., & Siegel, D. A. (2020). Metrics that matter for assessing the ocean biological carbon pump. *Proceedings of the National Academy of Sciences of the United States of America*, 117(18), 9679–9687. <https://doi.org/10.1073/pnas.1918114117>
- Campoverde, N. C. G., Hassenrück, C., Buttigieg, P. L., & Gärdes, A. (2018). Characterization of bacterioplankton communities and quantification of organic carbon pools off the Galapagos Archipelago under contrasting environmental conditions. *PeerJ*, 2018(12). <https://doi.org/10.7717/peerj.5984>
- Carini, P., Campbell, E. O., Morré, J., Sañudo-Wilhelmy, S. A., Cameron Thrash, J., Bennett, S. E., Temperton, B., Begley, T., & Giovannoni, S. J. (2014). Discovery of a SAR11 growth requirement for thiamin's pyrimidine precursor and its distribution in the Sargasso Sea. *ISME Journal*, 8(8), 1727–1738. <https://doi.org/10.1038/ismej.2014.61>
- Chen, J., Guo, K., Thornton, D. C. O., & Wu, Y. (2021). Effect of Temperature on the Release of Transparent Exopolymer Particles (TEP) and Aggregation by Marine Diatoms (*Thalassiosira weissflogii* and *Skeletonema marinoi*). *Journal of Ocean University of China*, 20(1), 56–66. <https://doi.org/10.1007/s11802-021-4528-3>

- Cianca, A., Godoy, J. M., Martin, J. M., Perez-Marrero, J., Rueda, M. J., Llinás, O., & Neuer, S. (2012). Interannual variability of chlorophyll and the influence of low-frequency climate modes in the North Atlantic subtropical gyre. *Global Biogeochemical Cycles*, 26(2). <https://doi.org/10.1029/2010GB004022>
- Cianca, Andrés, Helmke, P., Mouriño, B., Rueda, M. J., Llinás, O., & Neuer, S. (2007). Decadal analysis of hydrography and in situ nutrient budgets in the western and eastern North Atlantic subtropical gyre. *Journal of Geophysical Research: Oceans*, 112(7). <https://doi.org/10.1029/2006JC003788>
- Clarke, K. R., & Gorley, R. N. (2015). PRIMER v7 : *PRIMER-E Ltd Registered*, 296.
- Cotti-Rausch, B. E., Lomas, M. W., Lachenmyer, E. M., Baumann, E. G., & Richardson, T. L. (2020). Size-fractionated biomass and primary productivity of Sargasso Sea phytoplankton. *Deep-Sea Research Part I: Oceanographic Research Papers*, 156, 1–48. <https://doi.org/10.1016/j.dsr.2019.103141>
- Cotti-Rausch, B. E., Lomas, M. W., Lachenmyer, E. M., Goldman, E. A., Bell, D. W., Goldberg, S. R., & Richardson, T. L. (2016). Mesoscale and sub-mesoscale variability in phytoplankton community composition in the Sargasso Sea. *Deep-Sea Research Part I: Oceanographic Research Papers*, 110, 106–122. <https://doi.org/10.1016/j.dsr.2015.11.008>
- Cruz, B. N., Brozak, S., & Neuer, S. (2021a). Microscopy and DNA -based characterization of sinking particles at the Bermuda Atlantic Time-series Study station point to zooplankton mediation of particle flux . *Limnology and Oceanography*, 1–17. <https://doi.org/10.1002/lno.11910>
- Cruz, B. N., Brozak, S., & Neuer, S. (2021b). Microscopy and DNA-based characterization of sinking particles at the Bermuda Atlantic Time-series Study station point to zooplankton mediation of particle flux. *Limnology and Oceanography*, 66(10), 3697–3713. <https://doi.org/10.1002/lno.11910>
- Cruz, B. N., & Neuer, S. (2019). Heterotrophic bacteria enhance the aggregation of the marine picocyanobacteria prochlorococcus and synechococcus. *Frontiers in Microbiology*, 10(AUG), 1–11. <https://doi.org/10.3389/fmicb.2019.01864>
- Datta, M. S., Sliwerska, E., Gore, J., Polz, M. F., & Cordero, O. X. (2016). Microbial interactions lead to rapid micro-scale successions on model marine particles. *Nature Communications*, 7(May), 1–7. <https://doi.org/10.1038/ncomms11965>
- De Cáceres, M., Jansen, F., Dell, N. (2022). Package 'indicspecies'. URL <https://emf-creaf.github.io/indicspecies/>
- De Cáceres, M., Legendre, P., & Moretti, M. (2010). Improving indicator species analysis by combining groups of sites. *Oikos*, 119(10), 1674–1684. <https://doi.org/10.1111/j.1600-0706.2010.18334.x>
- De Martini, F., Neuer, S., Hamill, D., Robidart, J., & Lomas, M. W. (2018). Clade and strain specific contributions of Synechococcus and Prochlorococcus to carbon

export in the Sargasso Sea. *Limnology and Oceanography*, 63(2007), S448–S457. <https://doi.org/10.1002/lno.10765>

- Dortch, Q., & Packard, T. T. (1989). Differences in biomass structure between oligotrophic and eutrophic marine ecosystems. *Deep Sea Research Part A, Oceanographic Research Papers*, 36(2), 223–240. [https://doi.org/10.1016/0198-0149\(89\)90135-0](https://doi.org/10.1016/0198-0149(89)90135-0)
- Ducklow, H. W., Steinberg, D. K., William, C., Point, M. G., & Buesseler, K. O. (2001). Upper Ocean Carbon Export and the Biological Pump. Ducklow, H. W., Steinberg, D. K., William, C., Point, M. G., & Buesseler, K. O. (2001). Upper Ocean Carbon Export and the Biological Pump, 14(4). *Oceanography*, 14(4), 50–58.
- Dunn, O. J. (1961). Multiple Comparisons Among Means. *Journal of the American Statistical Association*, 56(293), 52. <https://doi.org/10.2307/2282330>
- Dupont, C. L., Mccrow, J. P., Valas, R., Moustafa, A., Walworth, N., Goodenough, U., Roth, R., Hogle, S. L., Bai, J., Johnson, Z. I., Mann, E., Palenik, B., Barbeau, K. A., Craig Venter, J., & Allen, A. E. (2015). Genomes and gene expression across light and productivity gradients in eastern subtropical Pacific microbial communities. *ISME Journal*, 9(5), 1076–1092. <https://doi.org/10.1038/ismej.2014.198>
- DuRand, M. D., Olson, R. J., & Chisholm, S. W. (2001). Phytoplankton population dynamics at the Bermuda Atlantic Time-series station in the Sargasso Sea. *Deep-Sea Research Part II: Topical Studies in Oceanography*, 48(8–9), 1983–2003. [https://doi.org/10.1016/S0967-0645\(00\)00166-1](https://doi.org/10.1016/S0967-0645(00)00166-1)
- Ewart, C. S., Meyers, M. K., Wallner, E. R., McGillicuddy, D. J., & Carlson, C. A. (2008). Microbial dynamics in cyclonic and anticyclonic mode-water eddies in the northwestern Sargasso Sea. *Deep-Sea Research Part II: Topical Studies in Oceanography*, 55(10–13), 1334–1347. <https://doi.org/10.1016/j.dsr2.2008.02.013>
- Fernández-Castro, B., Anderson, L., Marañón, E., Neuer, S., Ausín, B., González-Dávila, M., Santana-Casiano, J. M., Cianca, A., Santana, R., Llinás, O., Rueda, M. J., & Mouriño-Carballido, B. (2012). Regional differences in modelled net production and shallow remineralization in the North Atlantic subtropical gyre. *Biogeosciences*, 9(8), 2831–2846. <https://doi.org/10.5194/bg-9-2831-2012>
- Flintrop, C. M., Rogge, A., Miksch, S., Thiele, S., Waite, A. M., & Iversen, M. H. (2018). Embedding and slicing of intact in situ collected marine snow. *Limnology and Oceanography: Methods*, 16(6), 339–355. <https://doi.org/10.1002/lom3.10251>
- Flombaum, P., Wang, W. L., Primeau, F. W., & Martiny, A. C. (2020). Global picophytoplankton niche partitioning predicts overall positive response to ocean warming. *Nature Geoscience*, 13(2), 116–120. <https://doi.org/10.1038/s41561-019-0524-2>
- Fontanez, K. M., Eppley, J. M., Samo, T. J., Karl, D. M., & DeLong, E. F. (2015). Microbial community structure and function on sinking particles in the North Pacific Subtropical Gyre. *Frontiers in Microbiology*, 6(MAY), 1–14.

<https://doi.org/10.3389/fmicb.2015.00469>

- Frette, L., Jørgensen, N. O. G., Irming, H., & Kroer, N. (2004). *Tenacibaculum skagerrakense* sp. nov., a marine bacterium isolated from the pelagic zone in Skagerrak, Denmark. *International Journal of Systematic and Evolutionary Microbiology*, *54*(2), 519–524. <https://doi.org/10.1099/ijs.0.02398-0>
- García-Martín, E. E., Daniels, C. J., Davidson, K., Davis, C. E., Mahaffey, C., Mayers, K. M. J., McNeill, S., Poulton, A. J., Purdie, D. A., Tarran, G. A., & Robinson, C. (2019). Seasonal changes in plankton respiration and bacterial metabolism in a temperate shelf sea. *Progress in Oceanography*, *177*(December 2017), 101884. <https://doi.org/10.1016/j.pocean.2017.12.002>
- Gaube, P., Braun, C. D., Lawson, G. L., McGillicuddy, D. J., Penna, A. Della, Skomal, G. B., Fischer, C., & Thorrold, S. R. (2018). Mesoscale eddies influence the movements of mature female white sharks in the Gulf Stream and Sargasso Sea. *Scientific Reports*, *8*(1), 1–8. <https://doi.org/10.1038/s41598-018-25565-8>
- Giovannoni, S. J. (2017). SAR11 Bacteria: The Most Abundant Plankton in the Oceans. *Annual Review of Marine Science*, *9*(1), 231–255. <https://doi.org/10.1146/annurev-marine-010814-015934>
- Giovannoni, S. J., Cameron Thrash, J., & Temperton, B. (2014). Implications of streamlining theory for microbial ecology. *ISME Journal*, *8*(8), 1553–1565. <https://doi.org/10.1038/ismej.2014.60>
- Gloor, G. B., Macklaim, J. M., Pawlowsky-Glahn, V., & Egozcue, J. J. (2017). Microbiome datasets are compositional: And this is not optional. *Frontiers in Microbiology*, *8*(NOV), 1–6. <https://doi.org/10.3389/fmicb.2017.02224>
- Goldman, J. C. (1993). Potential role of large oceanic diatoms in new primary production. *Deep-Sea Research Part I*, *40*(1), 159–168. [https://doi.org/10.1016/0967-0637\(93\)90059-C](https://doi.org/10.1016/0967-0637(93)90059-C)
- Goldman, J. C., & McGillicuddy, D. J. (2003). Effect of large marine diatoms growing at low light on episodic new production. *Limnology and Oceanography*, *48*(3), 1176–1182. <https://doi.org/10.4319/lo.2003.48.3.1176>
- Gong, J., Qing, Y., Zou, S., Fu, R., Su, L., Zhang, X., & Zhang, Q. (2016). Protist-bacteria associations: Gammaproteobacteria and Alphaproteobacteria are prevalent as digestion-resistant bacteria in ciliated protozoa. *Frontiers in Microbiology*, *7*(APR), 1–16. <https://doi.org/10.3389/fmicb.2016.00498>
- Grossart, H. P., Kjørboe, T., Tang, K. W., Allgaier, M., Yam, E. M., & Ploug, H. (2006). Interactions between marine snow and heterotrophic bacteria: Aggregate formation and microbial dynamics. *Aquatic Microbial Ecology*, *42*(1), 19–26. <https://doi.org/10.3354/ame042019>
- Grossart, Hans Peter, Riemann, L., & Azam, F. (2001). Bacterial motility in the sea and its ecological implications. *Aquatic Microbial Ecology*, *25*(3), 247–258.

<https://doi.org/10.3354/ame025247>

- Gu erin, N., Ciccarella, M., Flamant, E., Fr emont, P., Mangenot, S., Istace, B., Noel, B., Romac, S., Bachy, C., Gachenot, M., Pelletier, E., Alberti, A., Jaillon, O., Cruaud, C., Wincker, P., Aury, J.-M., & Carradec, Q. (2021). Genomic adaptation of the picoeukaryote *Pelagomonas calceolata* to iron-poor oceans revealed by a chromosome-scale genome sequence. *BioRxiv*, 2021.10.25.465678. <https://www.biorxiv.org/content/10.1101/2021.10.25.465678v2%0Ahttps://www.biorxiv.org/content/10.1101/2021.10.25.465678v2.abstract>
- Guillou, L., Bachar, D., Audic, S., Bass, D., Berney, C., Bittner, L., Boutte, C., Burgaud, G., De Vargas, C., Decelle, J., Del Campo, J., Dolan, J. R., Dunthorn, M., Edvardsen, B., Holzmann, M., Kooistra, W. H. C. F., Lara, E., Le Bescot, N., Logares, R., ... Christen, R. (2013). The Protist Ribosomal Reference database (PR2): A catalog of unicellular eukaryote Small Sub-Unit rRNA sequences with curated taxonomy. *Nucleic Acids Research*, 41(D1), 597–604. <https://doi.org/10.1093/nar/gks1160>
- Guiry, M.D. and Guiry, G.M. (2012) Worldwide Electronic Publication. National University of Ireland, Gal-Way. <http://www.algaebase.org>
- Hansen, B., Verity, P., Falkenhaus, T., Tande, K. S., & Norrbin, F. (1994). On the trophic fate of *Phaeocystis pouchetti* (Harriot). V. Trophic relationships between *Phaeocystis* and zooplankton: An assessment of methods and size dependence. *Journal of Plankton Research*, 16(5), 487–511. <https://doi.org/10.1093/plankt/16.5.487>
- Hawley, A. K., Nobu, M. K., Wright, J. J., Durno, W. E., Morgan-Lang, C., Sage, B., Schwientek, P., Swan, B. K., Rinke, C., Torres-Beltr an, M., Mewis, K., Liu, W. T., Stepanauskas, R., Woyke, T., & Hallam, S. J. (2017). Diverse Marinimicrobia bacteria may mediate coupled biogeochemical cycles along eco-thermodynamic gradients. *Nature Communications*, 8(1), 1–9. <https://doi.org/10.1038/s41467-017-01376-9>
- Helmke, P., Neuer, S., Lomas, M. W., Conte, M., & Freudenthal, T. (2010). Cross-basin differences in particulate organic carbon export and flux attenuation in the subtropical North Atlantic gyre. *Deep-Sea Research Part I: Oceanographic Research Papers*, 57(2), 213–227. <https://doi.org/10.1016/j.dsr.2009.11.001>
- Holloway, G. (1986). Estimation of oceanic eddy transports from satellite altimetry. *Nature*, 323(6085), 243–244. <https://doi.org/10.1038/323243a0>
- Iversen, M. H., & Lampitt, R. S. (2020). Size does not matter after all: No evidence for a size-sinking relationship for marine snow. *Progress in Oceanography*, 189(November 2019). <https://doi.org/10.1016/j.pocean.2020.102445>
- Kim, S., Kang, I., Lee, J. W., Jeon, C. O., Giovannoni, S. J., & Cho, J. C. (2021). Heme auxotrophy in abundant aquatic microbial lineages. *Proceedings of the National Academy of Sciences of the United States of America*, 118(47).

<https://doi.org/10.1073/pnas.2102750118>

- Lambert, B. S., Fernandez, V. I., & Stocker, R. (2019). Motility drives bacterial encounter with particles responsible for carbon export throughout the ocean. *Limnology And Oceanography Letters*, 4(5), 113–118. <https://doi.org/10.1002/lol2.10113>
- Lavallée, B. F., & Pick, F. R. (2002). Picocyanobacteria abundance in relation to growth and loss rates in oligotrophic to mesotrophic lakes. *Aquatic Microbial Ecology*, 27(1), 37–46. <https://doi.org/10.3354/ame027037>
- Lomas, M. W., Bates, N. R., Johnson, R. J., Knap, A. H., Steinberg, D. K., & Carlson, C. A. (2013). Two decades and counting: 24-years of sustained open ocean biogeochemical measurements in the Sargasso Sea. *Deep-Sea Research Part II: Topical Studies in Oceanography*, 93, 16–32. <https://doi.org/10.1016/j.dsr2.2013.01.008>
- Lomas, Michael W., Bates, N. R., Johnson, R. J., Steinberg, D. K., & Tanioka, T. (2022). Adaptive carbon export response to warming in the Sargasso Sea. *Nature Communications*, 13(1), 1–10. <https://doi.org/10.1038/s41467-022-28842-3>
- Lomas, Michael W., Swain, A., Shelton, R., & Ammerman, J. W. (2004). Taxonomic variability of phosphorus stress in Sargasso Sea phytoplankton. *Limnology and Oceanography*, 49(6), 2303–2309. <https://doi.org/10.4319/lo.2004.49.6.2303>
- Lopes Dos Santos, A., Pollina, T., Gourvil, P., Corre, E., Marie, D., Garrido, J. L., Rodríguez, F., Noël, M. H., Vaultot, D., & Eikrem, W. (2017). Chloropicophyceae, a new class of picophytoplanktonic prasinophytes. *Scientific Reports*, 7(1), 1–20. <https://doi.org/10.1038/s41598-017-12412-5>
- Lynch, M. D. J., & Neufeld, J. D. (2015). Ecology and exploration of the rare biosphere. *Nature Reviews Microbiology*, 13(4), 217–229. <https://doi.org/10.1038/nrmicro3400>
- Makris, T. M., Makris, T. M., Sligar, S. G., Sligar, S. G., Schlichting, I., Schlichting, I., Mehn, M. P., Mehn, M. P., Jensen, M. P., Jensen, M. P., Zhang, R., Zhang, R., Newcomb, M., Newcomb, M., Clay, M. D., Clay, M. D., Solomon, E. I., Solomon, E. I., Behan, R. K., ... Schaffer, C. E. (2007). the Fe nucleus, thus decreasing d. In contrast, the removal of an electron from the redox-active ligand orbital has a minor effect on d (e.g., $d = -0.15$ mm/s for [Fe. *Science*, February, 838–840.
- Mari, X., Rassoulzadegan, F., Brussaard, C. P. D., & Wassmann, P. (2005). Dynamics of transparent exopolymeric particles (TEP) production by *Phaeocystis globosa* under N- or P-limitation: A controlling factor of the retention/export balance. *Harmful Algae*, 4(5), 895–914. <https://doi.org/10.1016/j.hal.2004.12.014>
- Mason, E., Pascual, A., & McWilliams, J. C. (2014). A new sea surface height-based code for oceanic mesoscale eddy tracking. *Journal of Atmospheric and Oceanic Technology*, 31(5), 1181–1188. <https://doi.org/10.1175/JTECH-D-14-00019.1>
- Mather, R. L., Reynolds, S. E., Wolff, G. A., Williams, R. G., Torres-Valdes, S.,

- Woodward, E. M. S., Landolfi, A., Pan, X., Sanders, R., & Achterberg, E. P. (2008). Phosphorus cycling in the North and South Atlantic Ocean subtropical gyres. *Nature Geoscience*, *1*(7), 439–443. <https://doi.org/10.1038/ngeo232>
- McGillicuddy, D. J. (2015). Formation of intrathermocline lenses by eddy-wind interaction. *Journal of Physical Oceanography*, *45*(2), 606–612. <https://doi.org/10.1175/JPO-D-14-0221.1>
- McGillicuddy, D. J., Kosnyrev, V. K., Ryan, J. P., & Yoder, J. A. (2001). Covariation of mesoscale ocean color and sea-surface temperature patterns in the Sargasso Sea. *Deep-Sea Research Part II: Topical Studies in Oceanography*, *48*(8–9), 1823–1836. [https://doi.org/10.1016/S0967-0645\(00\)00164-8](https://doi.org/10.1016/S0967-0645(00)00164-8)
- McGillicuddy, D. J., & Robinson, A. R. (1997). Eddy-induced nutrient supply and new production in the Sargasso Sea. *Deep-Sea Research Part I: Oceanographic Research Papers*, *44*(8), 1427–1450. [https://doi.org/10.1016/S0967-0637\(97\)00024-1](https://doi.org/10.1016/S0967-0637(97)00024-1)
- McGillicuddy, Dennis J. (2016). Mechanisms of Physical-Biological-Biogeochemical Interaction at the Oceanic Mesoscale. In *Annual Review of Marine Science* (Vol. 8, Issue September 2015). <https://doi.org/10.1146/annurev-marine-010814-015606>
- Mella-Flores, D., Six, C., Ratin, M., Partensky, F., Boutte, C., Le Corguillé, G., Marie, D., Blot, N., Gourvil, P., Kolowrat, C., & Garczarek, L. (2012). Prochlorococcus and synechococcus have evolved different adaptive mechanisms to cope with light and uv stress. *Frontiers in Microbiology*, *3*(AUG), 1–20. <https://doi.org/10.3389/fmicb.2012.00285>
- Mestre, M., Borrull, E., Sala, M., & Gasol, J. M. (2017). Patterns of bacterial diversity in the marine planktonic particulate matter continuum. *ISME Journal*, *11*(4), 999–1010. <https://doi.org/10.1038/ismej.2016.166>
- Moore, L. R., Ostrowski, M., Scanlan, D. J., Feren, K., & Sweetsir, T. (2005). Ecotypic variation in phosphorus-acquisition mechanisms within marine picocyanobacteria. *Aquatic Microbial Ecology*, *39*(3), 257–269. <https://doi.org/10.3354/ame039257>
- Morris, J. J., Johnson, Z. I., Szul, M. J., Keller, M., & Zinser, E. R. (2011). Dependence of the cyanobacterium Prochlorococcus on hydrogen peroxide scavenging microbes for growth at the ocean’s surface. *PLoS ONE*, *6*(2). <https://doi.org/10.1371/journal.pone.0016805>
- Morris, J. Jeffrey, Kirkegaard, R., Szul, M. J., Johnson, Z. I., & Zinser, E. R. (2008). Facilitation of robust growth of Prochlorococcus colonies and dilute liquid cultures by “helper” heterotrophic bacteria. *Applied and Environmental Microbiology*, *74*(14), 4530–4534. <https://doi.org/10.1128/AEM.02479-07>
- Morris, J. Jeffrey, Lenski, R. E., & Zinser, E. R. (2012). The black queen hypothesis: Evolution of dependencies through adaptive gene loss. *MBio*, *3*(2). <https://doi.org/10.1128/mBio.00036-12>

- Mouriño-Carballido, B. (2009). Eddy-driven pulses of respiration in the Sargasso Sea. *Deep-Sea Research Part I: Oceanographic Research Papers*, 56(8), 1242–1250. <https://doi.org/10.1016/j.dsr.2009.03.001>
- Mouriño-Carballido, B., & McGillicuddy, D. J. (2006). Mesoscale variability in the metabolic balance of the Sargasso Sea. *Limnology and Oceanography*, 51(6), 2675–2689. <https://doi.org/10.4319/lo.2006.51.6.2675>
- Needham, D. M., & Fuhrman, J. A. (2016). Pronounced daily succession of phytoplankton, archaea and bacteria following a spring bloom. *Nature Microbiology*, 1(4), 16005. <https://doi.org/10.1038/nmicrobiol.2016.5>
- Nelson, N. B., Siegel, D. A., & Yoder, J. A. (2004). The spring bloom in the northwestern Sargasso Sea: Spatial extent and relationship with winter mixing. *Deep-Sea Research Part II: Topical Studies in Oceanography*, 51(10-11 SPEC. ISS.), 987–1000. <https://doi.org/10.1016/j.dsr2.2004.02.001>
- Neuer, S., Davenport, R., Freudenthal, T., Wefer, G., Llinás, O., Rueda, M. J., Steinberg, D. K., & Karl, D. M. (2002). Differences in the biological carbon pump at three subtropical ocean sites. *Geophysical Research Letters*, 29(18). <https://doi.org/10.1029/2002GL015393>
- Neuer, S., Iversen, M., & Fischer, G. (2014). The Ocean's Biological Carbon pump as part of the global Carbon Cycle. *Limnology and Oceanography E-Lectures*, 4(4), 1–51. <https://doi.org/10.4319/lo.2014.sneuer.miversen.gfischer.9>
- Nian, R., Cai, Y., Zhang, Z., He, H., Wu, J., Yuan, Q., Geng, X., Qian, Y., Yang, H., & He, B. (2021). The Identification and Prediction of Mesoscale Eddy Variation via Memory in Memory With Scheduled Sampling for Sea Level Anomaly. *Frontiers in Marine Science*, 8(December). <https://doi.org/10.3389/fmars.2021.753942>
- Omand, M. M., Govindarajan, R., He, J., & Mahadevan, A. (2020). Sinking flux of particulate organic matter in the oceans: Sensitivity to particle characteristics. *Scientific Reports*, 10(1), 1–16. <https://doi.org/10.1038/s41598-020-60424-5>
- Oschlies, a, & Patzert, W. (2007). Eddy / Wind Interactions Stimulate. *Science*, 0(May), 1021–1026.
- Palter, J. B., Lozier, M. S., & Barber, R. T. (2005). The effect of advection on the nutrient reservoir in the North Atlantic subtropical gyre. *Nature*, 437(7059), 687–692. <https://doi.org/10.1038/nature03969>
- Parada, A. E., Needham, D. M., & Fuhrman, J. A. (2016). Every base matters: Assessing small subunit rRNA primers for marine microbiomes with mock communities, time series and global field samples. *Environmental Microbiology*, 18(5), 1403–1414. <https://doi.org/10.1111/1462-2920.13023>
- Parsons, R. J., Breitbart, M., Lomas, M. W., & Carlson, C. A. (2012). Ocean time-series reveals recurring seasonal patterns of virioplankton dynamics in the northwestern Sargasso Sea. *ISME Journal*, 6(2), 273–284. <https://doi.org/10.1038/ismej.2011.101>

- Partensky, F., Hess, W. R., & Vaultot, D. (1999). Prochlorococcus , a Marine Photosynthetic Prokaryote of Global Significance . *Microbiology and Molecular Biology Reviews*, 63(1), 106–127. <https://doi.org/10.1128/mubr.63.1.106-127.1999>
- Pascual, A., Faugère, Y., Larnicol, G., & Le Traon, P. Y. (2006). Improved description of the ocean mesoscale variability by combining four satellite altimeters. *Geophysical Research Letters*, 33(2), 2–5. <https://doi.org/10.1029/2005GL024633>
- Passow, U. (2002). Transparent exopolymer particles (TEP) in aquatic environments. *Progress in Oceanography*, 55(3–4), 287–333. [https://doi.org/10.1016/S0079-6611\(02\)00138-6](https://doi.org/10.1016/S0079-6611(02)00138-6)
- Passow, U., & Wassmann, P. (1994). On the trophic fate of *Phaeocystis pouchetii* (Hariot): IV. The formation of marine snow by *P. pouchetii*. *Marine Ecology Progress Series*, 104(1–2), 153–161. <https://doi.org/10.3354/meps104153>
- Pedrotti, M. L., Beauvais, S., Kerros, M. E., Iversen, K., & Peters, F. (2009). Bacterial colonization of transparent exopolymeric particles in mesocosms under different turbulence intensities and nutrient conditions. *Aquatic Microbial Ecology*, 55(3), 301–312. <https://doi.org/10.3354/ame01308>
- Pedrs-Ali, C. (2012). The rare bacterial biosphere. *Annual Review of Marine Science*, 4, 449–466. <https://doi.org/10.1146/annurev-marine-120710-100948>
- Piñeiro-Vidal, M., Riaza, A., & Santos, Y. (2008). *Tenacibaculum discolor* sp. nov. and *Tenacibaculum gallaicum* sp. nov., isolated from sole (*Solea senegalensis*) and turbot (*Psetta maxima*) culture systems. *International Journal of Systematic and Evolutionary Microbiology*, 58(1), 21–25. <https://doi.org/10.1099/ij.s.0.65397-0>
- Polovina, J. J., Howell, E. A., & Abecassis, M. (2008). Ocean’s least productive waters are expanding. *Geophysical Research Letters*, 35(3), 2–6. <https://doi.org/10.1029/2007GL031745>
- Quast, C., Pruesse, E., Yilmaz, P., Gerken, J., Schweer, T., Yarza, P., Peplies, J., & Glöckner, F. O. (2013). The SILVA ribosomal RNA gene database project: Improved data processing and web-based tools. *Nucleic Acids Research*, 41(D1), 590–596. <https://doi.org/10.1093/nar/gks1219>
- Raina, J. B., Lambert, B. S., Parks, D. H., Rinke, C., Siboni, N., Bramucci, A., Ostrowski, M., Signal, B., Lutz, A., Mendis, H., Rubino, F., Fernandez, V. I., Stocker, R., Hugenholtz, P., Tyson, G. W., & Seymour, J. R. (2022). Chemotaxis shapes the microscale organization of the ocean’s microbiome. *Nature*, 605(7908), 132–138. <https://doi.org/10.1038/s41586-022-04614-3>
- Richardson, K., & Bendtsen, J. (2017). Photosynthetic oxygen production in a warmer ocean: The Sargasso Sea as a case study. *Philosophical Transactions of the Royal Society A: Mathematical, Physical and Engineering Sciences*, 375(2102). <https://doi.org/10.1098/rsta.2016.0329>
- Richardson, P. L. (1983). Eddy Kinetic Energy in the North Atlantic From Surface

Drifters. *Journal of Geophysical Research*, 88(C7), 4355–4367.
<https://doi.org/10.1029/JC088iC07p04355>

- Robeson, M. S., O'Rourke, D. R., Kaehler, B. D., Ziemski, M., Dillon, M. R., Foster, J. T., & Bokulich, N. A. (2021). RESCRIPT: Reproducible sequence taxonomy reference database management. In *PLoS Computational Biology* (Vol. 17, Issue 11). <https://doi.org/10.1371/journal.pcbi.1009581>
- Rocap, G., Distel, D. L., Waterbury, J. B., & Chisholm, S. W. (2002). Resolution of *Prochlorococcus* and *Synechococcus* ecotypes by using 16S-23S ribosomal DNA internal transcribed spacer sequences. *Applied and Environmental Microbiology*, 68(3), 1180–1191. <https://doi.org/10.1128/AEM.68.3.1180-1191.2002>
- Rogge, A., Flintrop, C. M., Iversen, M. H., Salter, I., Fong, A. A., Vogts, A., & Waite, A. M. (2018). Hard and soft plastic resin embedding for single-cell element uptake investigations of marine-snow-associated microorganisms using nano-scale secondary ion mass spectrometry. *Limnology and Oceanography: Methods*, 16(8), 484–503. <https://doi.org/10.1002/lom3.10261>
- Romanenko, L. A., Tanaka, N., & Frolova, G. M. (2010). *Umboniibacter marinipunicus* gen. nov., sp. nov., a marine gammaproteobacterium isolated from the mollusc *Umbonium costatum* from the Sea of Japan. *International Journal of Systematic and Evolutionary Microbiology*, 60(3), 603–609. <https://doi.org/10.1099/ijs.0.010728-0>
- Scanlan, D. J., Ostrowski, M., Mazard, S., Dufresne, A., Garczarek, L., Hess, W. R., Post, A. F., Hagemann, M., Paulsen, I., & Partensky, F. (2009). Ecological Genomics of Marine Picocyanobacteria. *Microbiology and Molecular Biology Reviews*, 73(2), 249–299. <https://doi.org/10.1128/mnbr.00035-08>
- Schnitzer, A., & Steinberg, D. K. (2002). Natural diets of vertically migrating zooplankton in the Sargasso Sea. *Marine Biology*, 141(1), 89–99. <https://doi.org/10.1007/s00227-002-0815-8>
- Severns, P. M., & Sykes, E. M. (2020). Indicator species analysis: A useful tool for plant disease studies. *Phytopathology*, 110(12), 1860–1862. <https://doi.org/10.1094/PHYTO-12-19-0462-LE>
- Siegel, D. A. (1990). Meridional variations of the springtime phytoplankton community in the Sargasso Sea. *Journal of Marine Research*, 48(2), 379–412. <https://doi.org/10.1357/002224090784988791>
- Sjöstedt, J., Martiny, J. B. H., Munk, P., & Riemann, L. (2014). Abundance of broad bacterial taxa in the sargasso sea explained by environmental conditions but not water mass. *Applied and Environmental Microbiology*, 80(9), 2786–2795. <https://doi.org/10.1128/AEM.00099-14>
- Sohm, J. A., Ahlgren, N. A., Thomson, Z. J., Williams, C., Moffett, J. W., Saito, M. A., Webb, E. A., & Rocap, G. (2016). Co-occurring *Synechococcus* ecotypes occupy four major oceanic regimes defined by temperature, macronutrients and iron. *ISME Journal*, 10(2), 333–345. <https://doi.org/10.1038/ismej.2015.115>

- Steinberg, D. K., Carlson, C. A., Bates, N. R., Johnson, R. J., Michaels, A. F., & Knap, A. H. (2001). Overview of the US JGOFS Bermuda Atlantic Time-series Study (BATS): A decade-scale look at ocean biology and biogeochemistry. *Deep-Sea Research Part II: Topical Studies in Oceanography*, 48(8–9), 1405–1447. [https://doi.org/10.1016/S0967-0645\(00\)00148-X](https://doi.org/10.1016/S0967-0645(00)00148-X)
- Stockner, J. G. (1988). Phototrophic picoplankton: An overview from marine and freshwater ecosystems. *Limnology and Oceanography*, 33(4part2), 765–775. <https://doi.org/10.4319/lo.1988.33.4part2.0765>
- Suttle, C., Chan, A., & Fuhrman, J. (1991). Dissolved free amino acids in the Sargasso Sea: uptake and respiration rates, turnover times, and concentrations. *Marine Ecology Progress Series*, 70(July 1988), 189–199. <https://doi.org/10.3354/meps070189>
- Sweeney, E. N., McGillicuddy, D. J., & Buesseler, K. O. (2003). Biogeochemical impacts due to mesoscale eddy activity in the Sargasso Sea as measured at the Bermuda Atlantic Time-series Study (BATS). *Deep-Sea Research Part II: Topical Studies in Oceanography*, 50(22–26), 3017–3039. <https://doi.org/10.1016/j.dsr2.2003.07.008>
- Tang, K. W., Jakobsen, H. H., & Visser, A. W. (2001). *Phaeocystis globosa* (Prymnesiophyceae) and the planktonic food web: Feeding, growth, and trophic interactions among grazers. *Limnology and Oceanography*, 46(8), 1860–1870. <https://doi.org/10.4319/lo.2001.46.8.1860>
- Tanković, M. S., Baričević, A., Ivančić, I., Kužat, N., Medić, N., Pustijanac, E., Novak, T., Gašparović, B., Pfannkuchen, D. M., & Pfannkuchen, M. (2018). Insights into the life strategy of the common marine diatom *Chaetoceros peruvianus* Brightwell. *PLoS ONE*, 13(9), 1–21. <https://doi.org/10.1371/journal.pone.0203634>
- Tansel, B. (2018). Morphology, composition and aggregation mechanisms of soft bioflocs in marine snow and activated sludge: A comparative review. *Journal of Environmental Management*, 205, 231–243. <https://doi.org/10.1016/j.jenvman.2017.09.082>
- Thrash, J. C., Seitz, K. W., Baker, B. J., Temperton, B., Gillies, L. E., Rabalais, N. N., Henrissat, B., & Mason, O. U. (2017). Metabolic roles of uncultivated bacterioplankton lineages in the northern gulf of Mexico “dead zone.” *MBio*, 8(5). <https://doi.org/10.1128/mBio.01017-17>
- Treusch, A. H., Demir-Hilton, E., Vergin, K. L., Worden, A. Z., Carlson, C. A., Donatz, M. G., Burton, R. M., & Giovannoni, S. J. (2012). Phytoplankton distribution patterns in the northwestern Sargasso Sea revealed by small subunit rRNA genes from plastids. *ISME Journal*, 6(3), 481–492. <https://doi.org/10.1038/ismej.2011.117>
- Troussellier, M., Escalas, A., Bouvier, T., & Mouillot, D. (2017). Sustaining rare marine microorganisms: Macroorganisms as repositories and dispersal agents of microbial diversity. *Frontiers in Microbiology*, 8(MAY), 1–17.

<https://doi.org/10.3389/fmicb.2017.00947>

- Ustick, L. J., Larkin, A. A., Garcia, C. A., Garcia, N. S., Brock, M. L., Lee, J. A., Wiseman, N. A., Keith Moore, J., & Martiny, A. C. (2021). Metagenomic analysis reveals global-scale patterns of ocean nutrient limitation. *Science*, *372*(6539), 287–291. <https://doi.org/10.1126/science.abe6301>
- Verdugo, P. (2012). Marine microgels. *Annual Review of Marine Science*, *4*, 375–400. <https://doi.org/10.1146/annurev-marine-120709-142759>
- Verhoeven, K. J. F., Simonsen, K. L., & McIntyre, L. (2005). Erratum: Implementing false discovery rate control: Increasing your power (*Oikos* (2005) 108 (643-647)). *Oikos*, *109*(1), 208. <https://doi.org/10.1111/j.0030-1299.2005.13426.x>
- Villacorte, L. O., Ekowati, Y., Calix-Ponce, H. N., Schippers, J. C., Amy, G. L., & Kennedy, M. D. (2015). Improved method for measuring transparent exopolymer particles (TEP) and their precursors in fresh and saline water. *Water Research*, *70*(April 2018), 300–312. <https://doi.org/10.1016/j.watres.2014.12.012>
- Villareal, T. A., Woods, S., Moore, J. K., & Culver-Rymsza, K. (1996). Vertical migration of *Rhizosolenia* mats and their significance to NO₃⁻ fluxes in the central North Pacific gyre. *Journal of Plankton Research*, *18*(7), 1103–1121. <https://doi.org/10.1093/plankt/18.7.1103>
- Wald, A. (1943). Tests of Statistical Hypotheses Concerning Several Parameters When the Number of Observations is Large. *Transactions of the American Mathematical Society*, *54*(3), 426. <https://doi.org/10.2307/1990256>
- Wilson, S. E., & Steinberg, D. K. (2010). Autotrophic picoplankton in mesozooplankton guts: Evidence of aggregate feeding in the mesopelagic zone and export of small phytoplankton. *Marine Ecology Progress Series*, *412*, 11–27. <https://doi.org/10.3354/meps08648>
- Woeckel, D., Fuchs, B. M., Kuypers, M. M. M., & Amann, R. (2007). Potential interactions of particle-associated anammox bacteria with bacterial and archaeal partners in the Namibian upwelling system. *Applied and Environmental Microbiology*, *73*(14), 4648–4657. <https://doi.org/10.1128/AEM.02774-06>
- Worden, A. Z., Janouskovec, J., McRose, D., Engman, A., Welsh, R. M., Malfatti, S., Tringe, S. G., & Keeling, P. J. (2012). Global distribution of a wild alga revealed by targeted metagenomics. *Current Biology*, *22*(17), R675–R677. <https://doi.org/10.1016/j.cub.2012.07.054>
- Yeh, Y. C., McNichol, J., Needham, D. M., Fichot, E. B., Berdjeb, L., & Fuhrman, J. A. (2021). Comprehensive single-PCR 16S and 18S rRNA community analysis validated with mock communities, and estimation of sequencing bias against 18S. *Environmental Microbiology*, *23*(6), 3240–3250. <https://doi.org/10.1111/1462-2920.15553>

Zinser, E. R. (2018). Cross-protection from hydrogen peroxide by helper microbes: the impacts on the cyanobacterium *Prochlorococcus* and other beneficiaries in marine communities. *Environmental Microbiology Reports*, 10(4), 399–411.
<https://doi.org/10.1111/1758-2229.12625>

APPENDIX A

TABLES

Table 1: Sampling dates and station locations. A three-day deployment of poisoned particle interceptor traps (PITs) at 150 m depth was done for each station. Ambient seawater was collected after the PITs deployments and recoveries at 20 m and the deep chlorophyll maximum that ranged in depth from 80 to 100 m.

	Season	Station	PITs Deployment	PITs Recovery	Latitude	Longitude
AE1206	Spring 2012	BATS	15 March	17 March	32° 50'N	63° 30'W
		C2	19 March	21 March	31° 40'N	64° 10'W
AE1219	Summer 2012	AC2	20 July	22 July	33° 30'N	64° 27'W
		Ace2	24 July	26 July	32° 22'N	64° 22'W
		BATS	28 July	30 July	31° 40'N	64° 10'W

Table 2: Sample information, feature counts, and alpha-diversity indices of prokaryotes and photoautotrophs. Samples from 150 m are from sediment traps.

Station	Sample ID	Depth	Sequence Counts	Prokaryotes		Photoautotrophs	
				Observed Features	Shannon's Index	Observed Features	Shannon's Index
C2	173	20	37995	337	5.06	82	2.70
	175	80	51116	453	6.52	95	3.76
	202	20	49064	299	4.09	76	2.20
	205	100	55807	574	7.73	86	4.44
	222	150	11099	290	7.03	100	5.54
	223	150	8250	208	5.20	79	3.94
BATS (B3)	232	20	35858	370	6.28	97	3.69
	234	80	56788	523	7.14	82	3.26
	253	20	31018	310	5.96	87	3.24
	258	100	31806	638	8.21	41	4.34
	283	150	1549	–	–	–	–
	284*	150	–	–	–	–	–
AC2	288†	20	10	–	–	–	–
	290*	85	–	–	–	–	–
	316	20	31600	250	6.04	88	2.83
	319	110	69393	259	8.07	122	5.03
	346	150	11218	353	5.85	77	5.05
	347	150	11511	439	5.48	71	4.62
Ace2	348	20	54347	390	5.93	89	2.29
	351	100	38611	555	6.94	72	3.04
	376	20	58222	215	5.87	104	2.48
	379	100	43031	283	7.94	63	4.69
	398	150	17515	362	4.47	70	4.67
	399	150	14899	578	5.08	61	5.13
BATS (B4)	406	20	56840	291	6.38	99	3.03
	409	95	39092	583	7.79	103	4.91
	438	20	37490	267	6.65	94	3.57
	441	100	53130	802	7.41	105	4.93
	442*	150	–	–	–	–	–
	443†	150	769	–	–	–	–

†Low sample size

*Missing sample

–Missing value

Table 3: Pairwise permutational multivariate analysis of variance based on Bray-Curtis dissimilarities from the rarefied abundance of prokaryotes. The table shows comparisons of the effect of seasonality (spring & fall), depth (20m, DCM & PITs), eddy (C2, B3, AC2, Ace2 and B4), and sample type (Seawater & PITs). Samples were filtered by sample type to apply the PERMANOVA test. All samples compared were $n > 4$. The asterisk indicates significant differences (FDR-corrected, $p < 0.05$) between sample groups.

Predictor	Seawater			PITs			Seawater & PITs		
	R ²	p-value	FDR	R ²	p-value	FDR	R ²	p-value	FDR
Season	0.228	0.004	0.009*	0.433	0.067	0.089	0.159	0.001	0.003*
Depth	0.258	0.001	0.003*	–	–	–	0.359	0.001	0.003*
Location	0.372	0.034	0.052	0.819	0.067	0.089	0.315	0.003	0.008*
Sample Type	–	–	–	–	–	–	0.503	0.001	0.003*
Depth (Spring)	0.349	0.034	0.052	–	–	–	0.587	0.001	0.003*
Depth (Summer)	0.491	0.015	0.030*	–	–	–	0.151	0.196	0.230
Location (Spring)	0.201	0.207	0.230	–	–	–	0.199	0.199	0.230
Location (Summer)	0.180	0.542	0.542	0.900	0.333	0.351	0.220	0.001	0.003*
Sample Type (Spring)	–	–	–	–	–	–	0.312	0.029	0.052
Sample Type (Summer)	–	–	–	–	–	–	0.355	0.003	0.008*

Table 4: Pairwise permutational multivariate analysis of variance based on Bray-Curtis dissimilarities from the rarefied abundances of photoautotrophs. The table shows comparisons of the effect of seasonality (spring & fall), depth (20m, DCM & PITs), eddy (C2, B3, AC2, Ace2 and B4), and sample type (Seawater & PITs). Samples were filtered by sample type to apply the PERMANOVA test. All samples compared were $n > 4$. The asterisk indicates significant differences (FDR-corrected, $p < 0.05$) between sample group.

Predictors	Seawater			PITs			Seawater & PITs		
	R ²	p-value	FDR	R ²	p-value	FDR	R ²	p-value	FDR
Season	0.323	0.002	0.008*	0.507	0.067	0.089	0.245	0.001	0.005*
Depth	0.269	0.001	0.005*	–	–	–	0.349	0.001	0.005*
Location	0.412	0.019	0.035*	0.707	0.067	0.089	0.350	0.003	0.009*
Sample Type	–	–	–	–	–	–	0.171	0.005	0.011*
Depth (Spring)	0.326	0.034	0.057	–	–	–	0.448	0.003	0.009*
Depth (Summer)	0.589	0.015	0.030*	–	–	–	0.661	0.001	0.005*
Location (Spring)	0.149	0.459	0.493	–	–	–	0.117	0.468	0.493
Location (Summer)	0.127	0.659	0.659	0.625	0.333	0.417	0.146	0.457	0.493
Sample Type (Spring)	–	–	–	–	–	–	0.251	0.047	0.072
Sample Type (Summer)	–	–	–	–	–	–	0.312	0.004	0.010*

Table 5: Prokaryote Indicator Species Analysis indicating generalist taxa and significant (FDR $p < 0.05$) seawater indicators (IndVal ≥ 0.8). The upper panel indicates generalist taxa, i.e., found within all tested sample groups, and the lower panel indicators of seawater.

Taxon	PITs	PITs	SW	SW	Index	IndVal	p-value	FDR
	Spring	Summer	Spring	Summer				
<i>Prochlorococcus</i> MIT9313	1	1	1	1	15	1	–	–
SAR116 clade	1	1	1	1	15	1	–	–
<i>Rhodobacterales</i> ; <i>Rhodobacteraceae</i>	1	1	1	1	15	1	–	–
<i>Alphaproteobacteria</i> ; SAR11 Clade Ia	1	1	1	1	15	1	–	–
<i>Alteromonas</i>	1	1	1	1	15	1	–	–
<i>Marinimicrobia</i> ; SAR406 clade	1	1	1	1	15	1	–	–
<i>Flavobacteriaceae</i> ; NS2b marine group	1	1	1	1	15	1	–	–
<i>Cyanobium</i> PCC 6307	1	1	1	1	15	1	–	–
<i>Synechococcus</i> CC9902	1	1	1	1	15	1	–	–
<i>Alphaproteobacteria</i> ; <i>Rickettsiales</i> ; S25 593	0	0	1	1	10	1	0.0001	0.003
<i>Pseudomonadales</i> ; OM182 clade	0	0	1	1	10	1	0.0001	0.003
<i>Pseudomonadales</i> ; SAR86 clade	0	0	1	1	10	1	0.0001	0.003
SAR11 Clade III	0	0	1	1	10	0.972	0.0004	0.005
<i>Alphaproteobacteria</i> ; SAR11 Clade I	0	0	1	1	10	0.943	0.0012	0.017
SAR92 clade	0	0	1	1	10	0.943	0.0013	0.018
<i>Dadabacteriales</i>	0	0	1	1	10	0.943	0.0015	0.020
<i>Rhodospirillales</i> ; <i>Magnetospiraceae</i>	0	0	1	1	10	0.913	0.0016	0.021
<i>Myxococcales</i> ; <i>Myxococcaceae</i> P3OB 42	0	0	1	1	10	0.913	0.0018	0.023
<i>Rhodospirillales</i> ; AEGEAN 169 marine group	0	0	1	1	10	0.936	0.0107	0.065
<i>Gammaproteobacteria</i> ; Ga0077536	0	0	1	1	10	0.882	0.0119	0.067
<i>Thermoplasmata</i> (Marine Group II)	0	0	1	1	10	0.913	0.0126	0.070

Table 6: Indicator Species Analysis of photoautotrophs indicating generalist taxa and significant (FDR, $p < 0.05$) seawater indicators (IndVal ≥ 0.8). The upper panel indicates generalist taxa, i.e., found within all tested sample groups, and the lower panel

Taxon	PITS Spring	PITs Summer	SW Spring	SW Summer	IndVal	p-value	FDR p-value
<i>Prochlorococcus</i> MIT9313	1	1	1	1	1.00	–	–
<i>Emiliana huxleyi</i>	1	1	1	1	1.00	–	–
<i>Prymnesiales</i>	1	1	1	1	1.00	–	–
<i>Prymnesiophyceae</i>	1	1	1	1	1.00	–	–
<i>Phaeocystis</i> sp.	1	1	1	1	1.00	–	–
<i>Synechococcus</i> CC9902	1	1	1	1	1.00	–	–
<i>Cyanobiaceae</i>	1	1	1	1	0.98	–	–
<i>Dictyochophyceae</i>	1	1	1	1	0.96	–	–
<i>Bacillariophyta</i>	1	1	1	1	0.94	–	–
<i>Sarcinochrysidaceae</i>	1	1	1	1	0.94	–	–
<i>Chrysochromulina camella</i>	1	1	1	1	0.91	–	–
<i>Pelagomonas</i> sp.	1	1	1	1	0.91	–	–
<i>Braarudosphaeraceae</i>	1	1	1	1	0.76	–	–
<i>Florenciella parvula</i>	0	0	1	1	0.82	0.05	0.15
<i>Chrysochromulinaceae</i>	0	0	1	1	0.78	0.10	0.23
<i>Bathycoccus prasinus</i>	0	0	1	1	0.74	0.25	0.41
<i>Ostreococcus</i>	0	0	1	1	0.67	0.29	0.42
<i>Ochrophyta</i>	0	0	1	1	0.41	0.90	0.99
<i>Prymnesiophyceae</i>	0	0	1	1	0.33	1.00	1.00

APPENDIX B

FIGURES

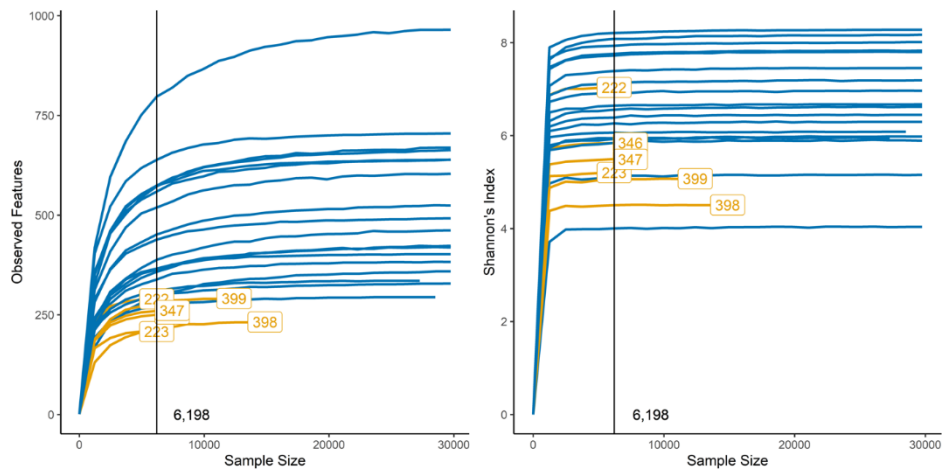


Figure 1: Species-saturation curves of prokaryotes based on the alpha-diversity estimators (A) Observed Features and (B) Shannon's Index as a function of sampling effort for 16S rRNA gene amplicon libraries within the seawater (blue) and trap material (brown). The black vertical line represents the library size depth (6,198) used to rarefy the SILVA-based ASV table.

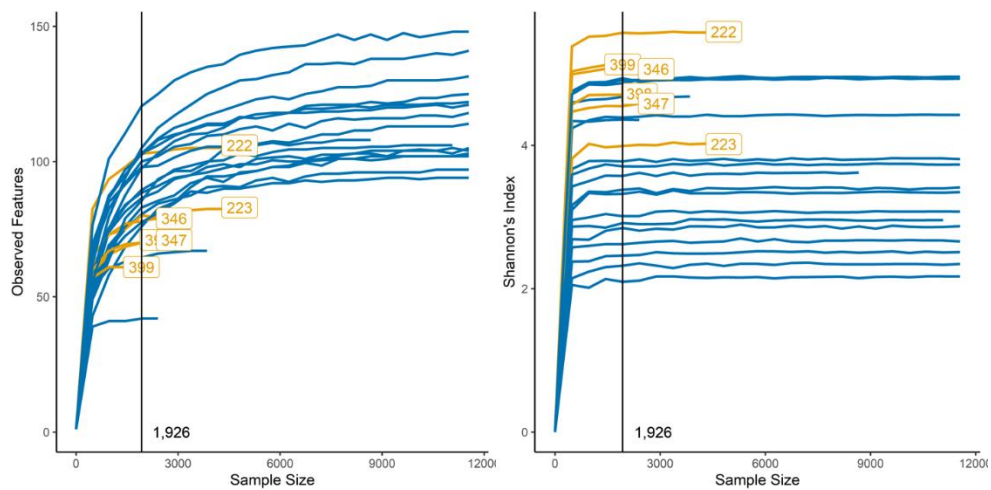


Figure 2: Species-saturation curves of phototrophs based on the alpha-diversity estimators (A) Observed Features and (B) Shannon's Index as a function of sampling effort for 16S rRNA gene amplicon libraries within the seawater (blue) and trap material (brown). The black vertical line represents the library size depth (6,198) used to rarefy the PR²-based ASV table.

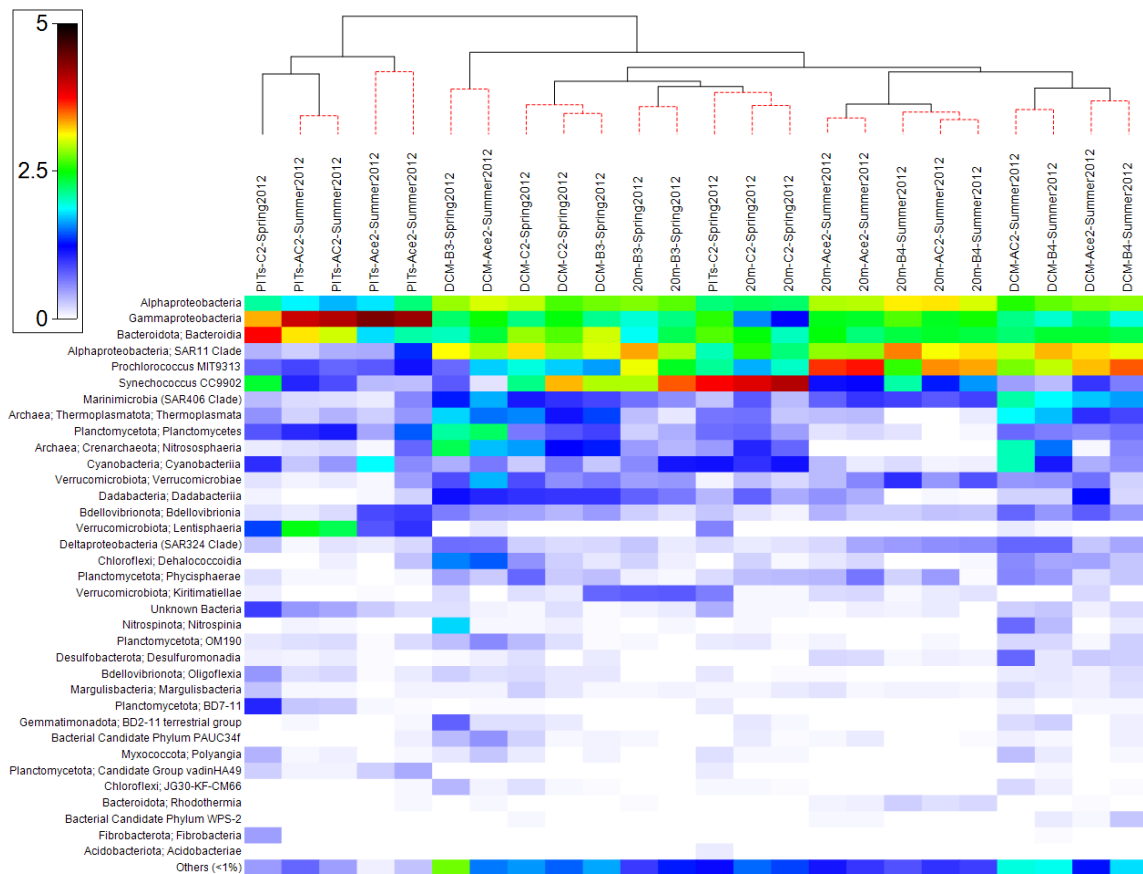


Figure 3: Log($x + 1$)-transformed relative abundance of prokaryotic classes. The dendrogram represents the compositional dissimilarity between samples using UPGMA for hierarchical clustering. Black lines represent significant differences between clusters (SIMPROF, $p < 0.05$), and red dashed lines represent significant similarity (SIMPROF, $p \geq 0.05$). Taxa not represented in at least 1% of the total community in each sample were grouped into the “*Others*” category.

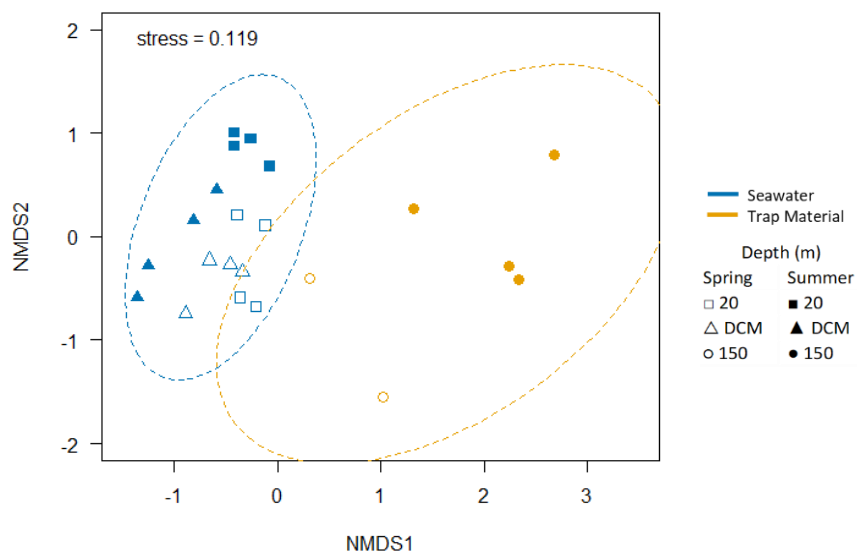


Figure 4: Non-metric Multidimensional Scaling (NMDS) ordination of Bray-Curtis dissimilarity based on the compositional differences of the prokaryotic community in seawater (blue) and trap material (brown) during spring (filled symbols) and summer (unfilled symbols) samples collected at four different depths (symbol shape). Dashed lines represent 95% confidence ellipses.

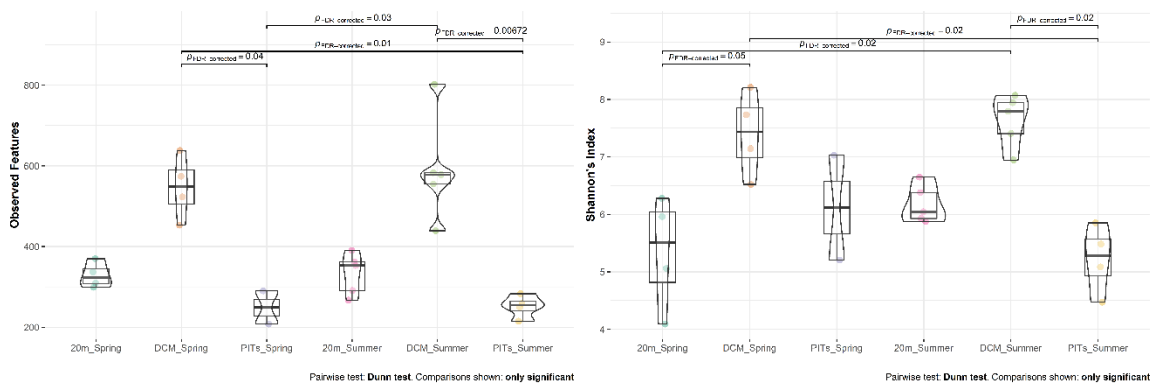


Figure 5: Alpha-diversity metrics of the gene amplicon libraries of prokaryotes plotted as violin plots overlaid to box and whiskers plots showing both distribution and variations of (A) Observed Features and (B) Shannon's Index. Metrics were plotted as a function of depth for Spring 2012 and Summer 2012. Samples represent the upper 20m, Deep Chlorophyll Maxima (DCM) and trap material collected at 150m (PITs). The FDR-corrected *p-value* represent pairwise group significance of samples that are significantly different.

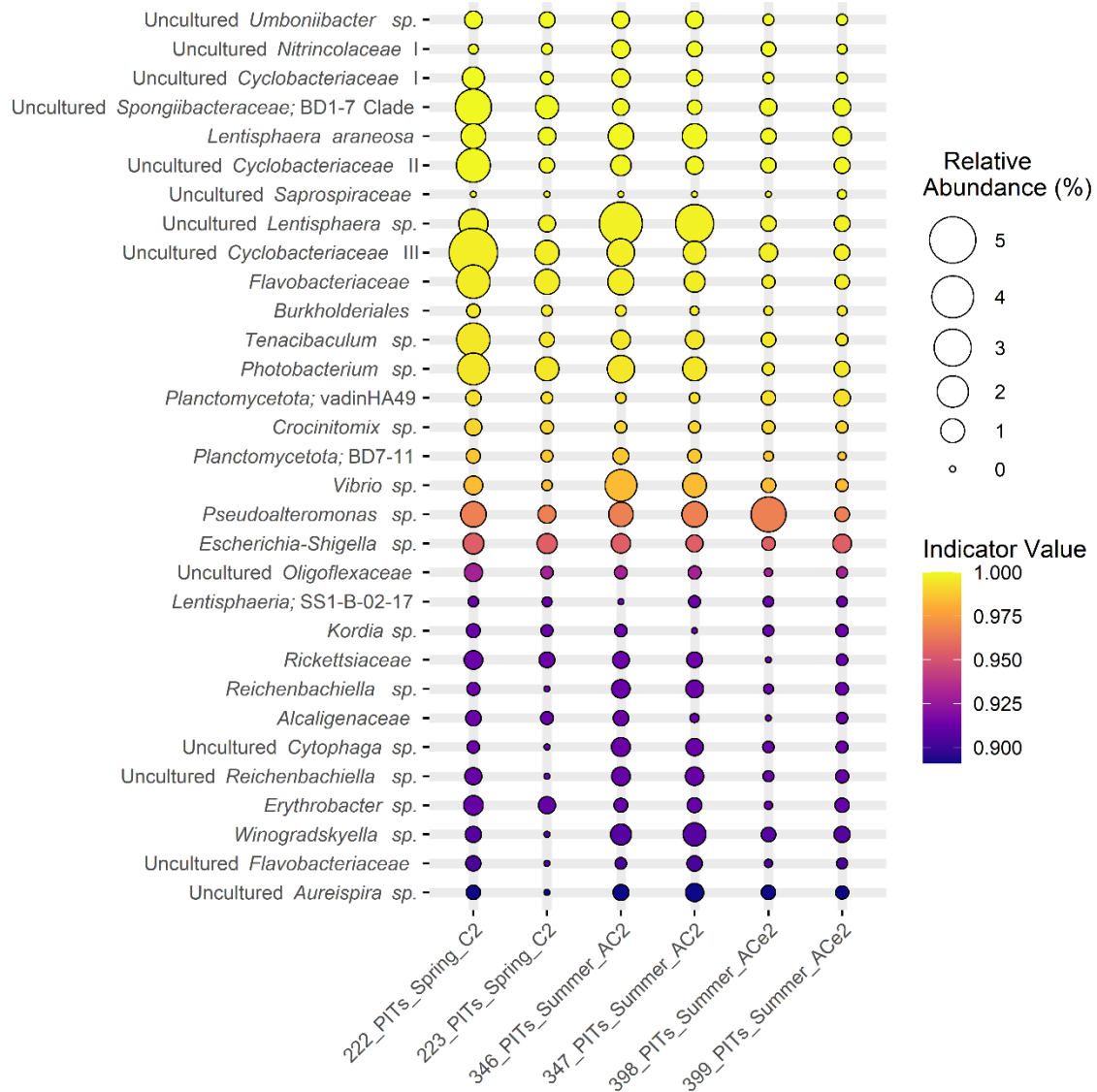


Figure 6: Balloon plot depicting relative abundance of significant prokaryotic indicator taxa ($p < 0.05$) for the trap material collected in spring and summer. The size of the bubbles depicts the relative percent abundance for each sample and the color shows indicator value range. Significant value ≤ 0.8 were considered as indicators.

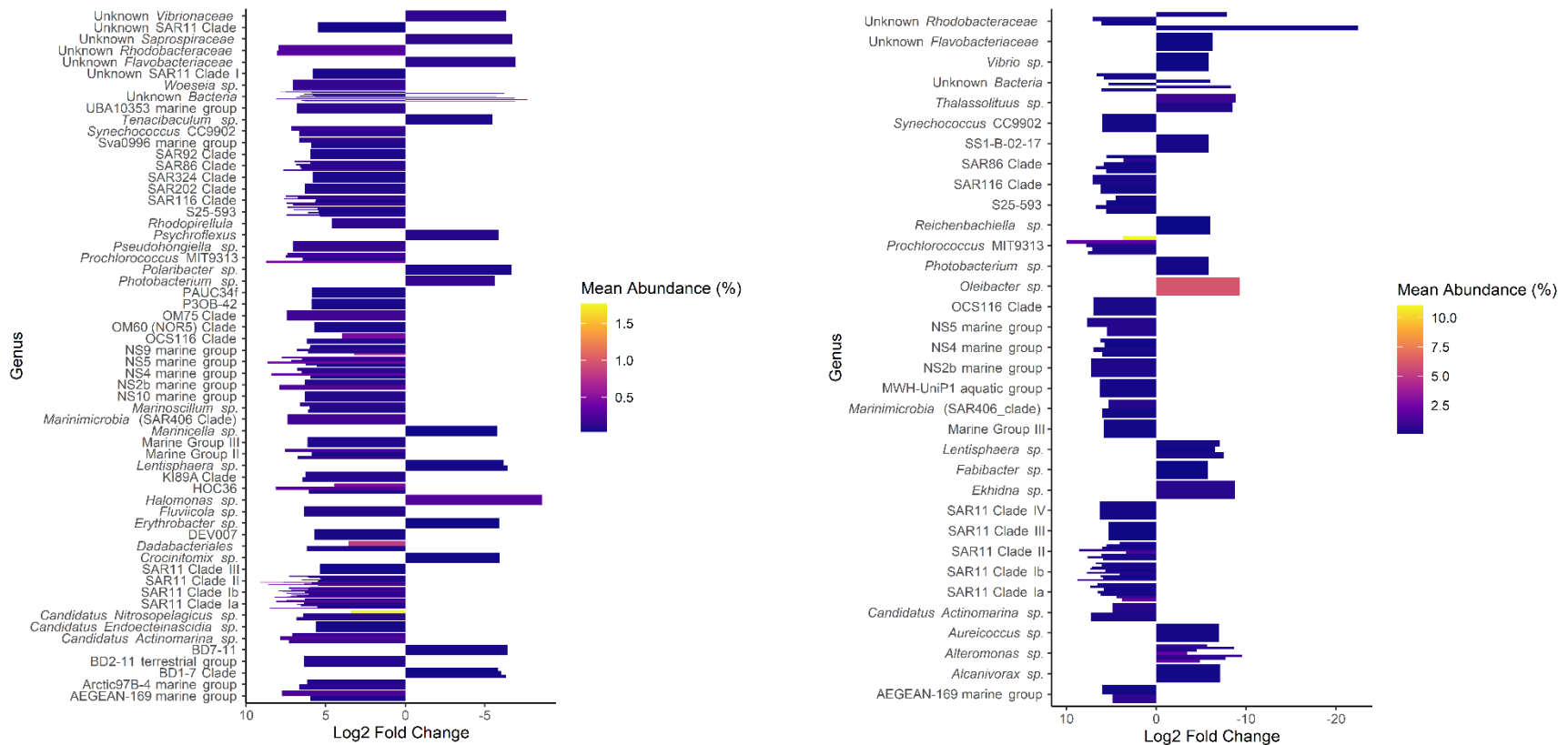


Figure 7: Difference in abundance of prokaryotes expressed as significant (FDR, $p < 0.05$) fold change between normalized taxonomic counts in seawater (positive values) and trap material (negative values) from the (A) spring and (B) summer seasons. The color represents the average abundance of mean normalized counts in all samples.

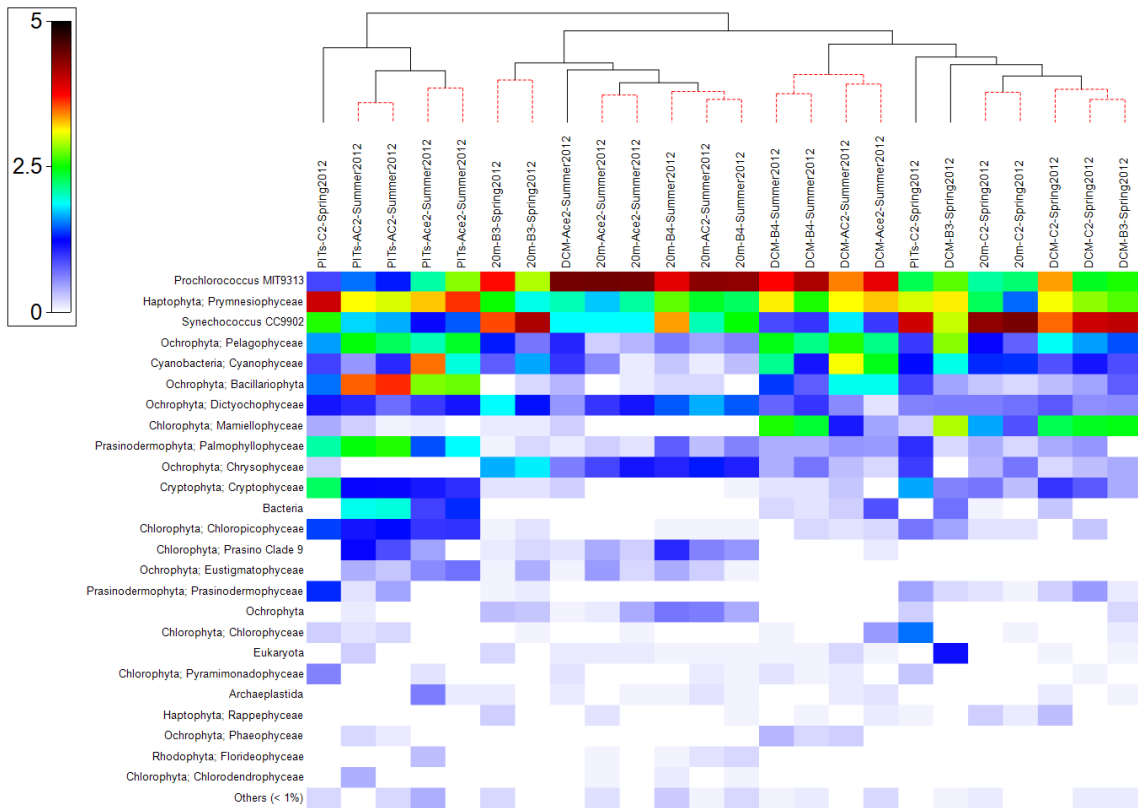


Figure 8: $\text{Log}(x + 1)$ -transformed relative abundance of photoautotrophic orders. The dendrogram represents the compositional dissimilarity between samples using UPGMA for hierarchical clustering. Black lines represent significant differences between clusters (SIMPROF, $p < 0.05$), and red dashed lines represent significant similarity (SIMPROF, $p \geq 0.05$). Taxa not represented in at least 1% of the total community in each sample were grouped into the “Others” category.

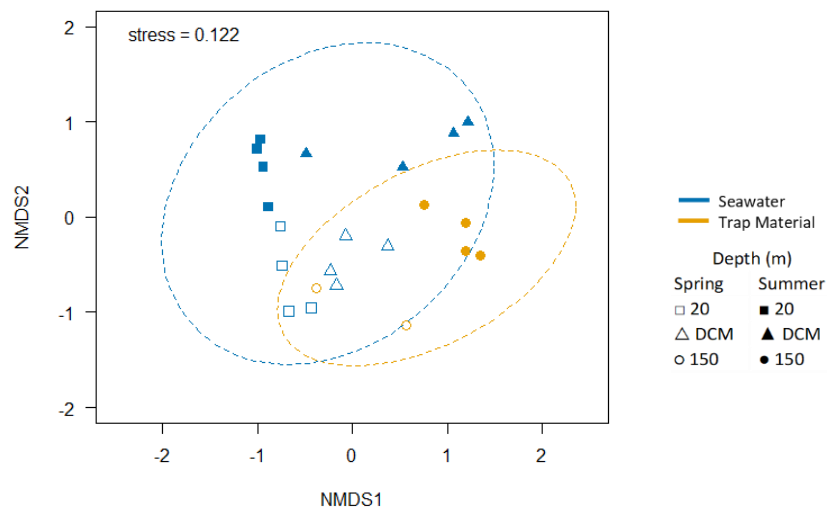


Figure 9: Non-metric Multidimensional Scaling (NMDS) ordination of Bray-Curtis dissimilarity based on the compositional differences of the photoautotrophic community in seawater (blue) and trap material (brown) during spring (filled symbols) and summer (unfilled symbols) samples collected at four different depths (symbol shape). Dashed lines represent 95% confidence ellipses.

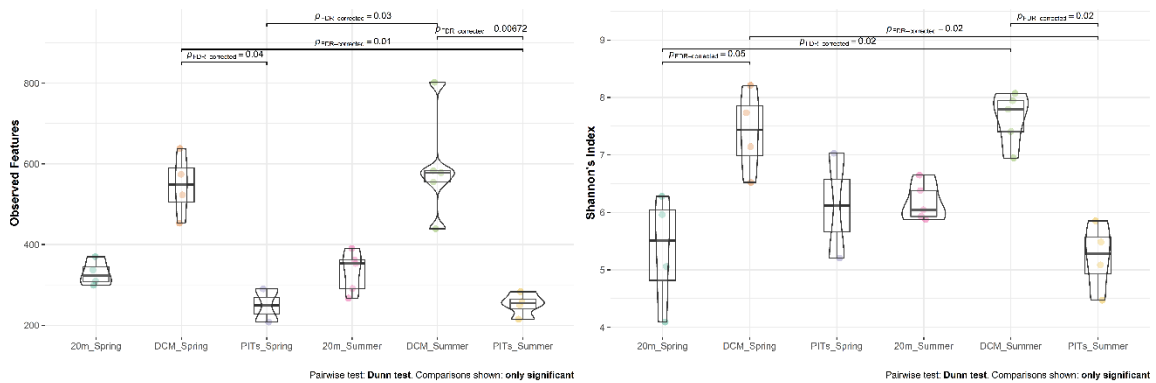


Figure 10: Alpha-diversity metrics of the gene amplicon libraries of photoautotrophs plotted as violin plots overlaid to box and whiskers plots showing both distribution and variations of (A) Observed Features and (B) Shannon's Index. Metrics were plotted as a function of depth for Spring 2012 and Summer 2012. Samples represent the upper 20m, Deep Chlorophyl Maxima (DCM) and trap material collected at 150m (PITs). The FDR-corrected *p-value* represent pairwise group significance of samples that are significantly different.

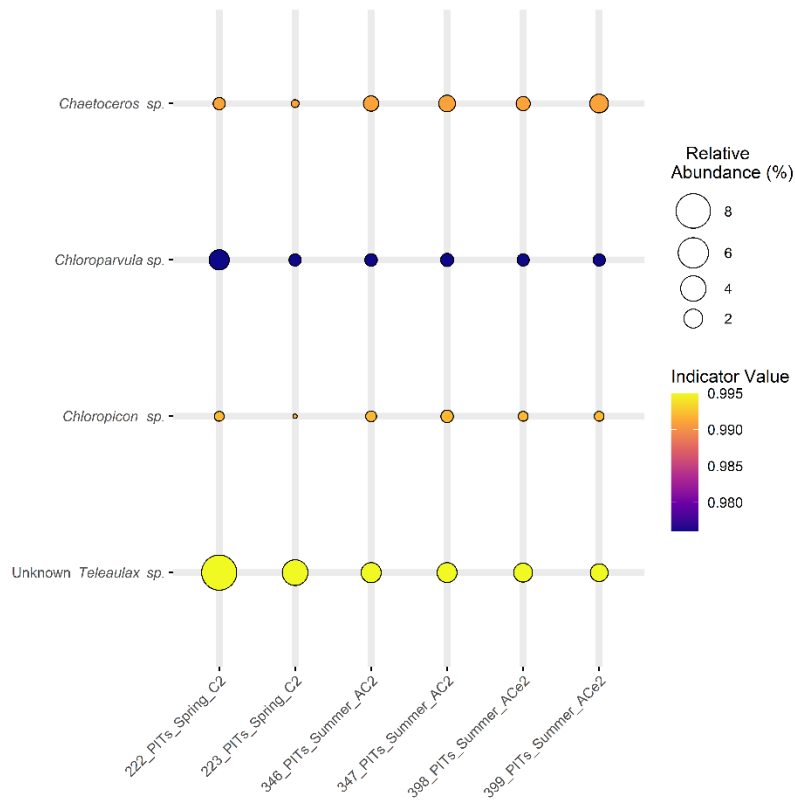


Figure 11: Balloon plot depicting relative abundance of significant photoautotrophic indicator taxa ($p < 0.05$) for the trap material collected in spring and summer. The size of the bubbles depicts the relative percent abundance for each sample and the color shows indicator value range. Significant value ≤ 0.8 were considered as indicators.

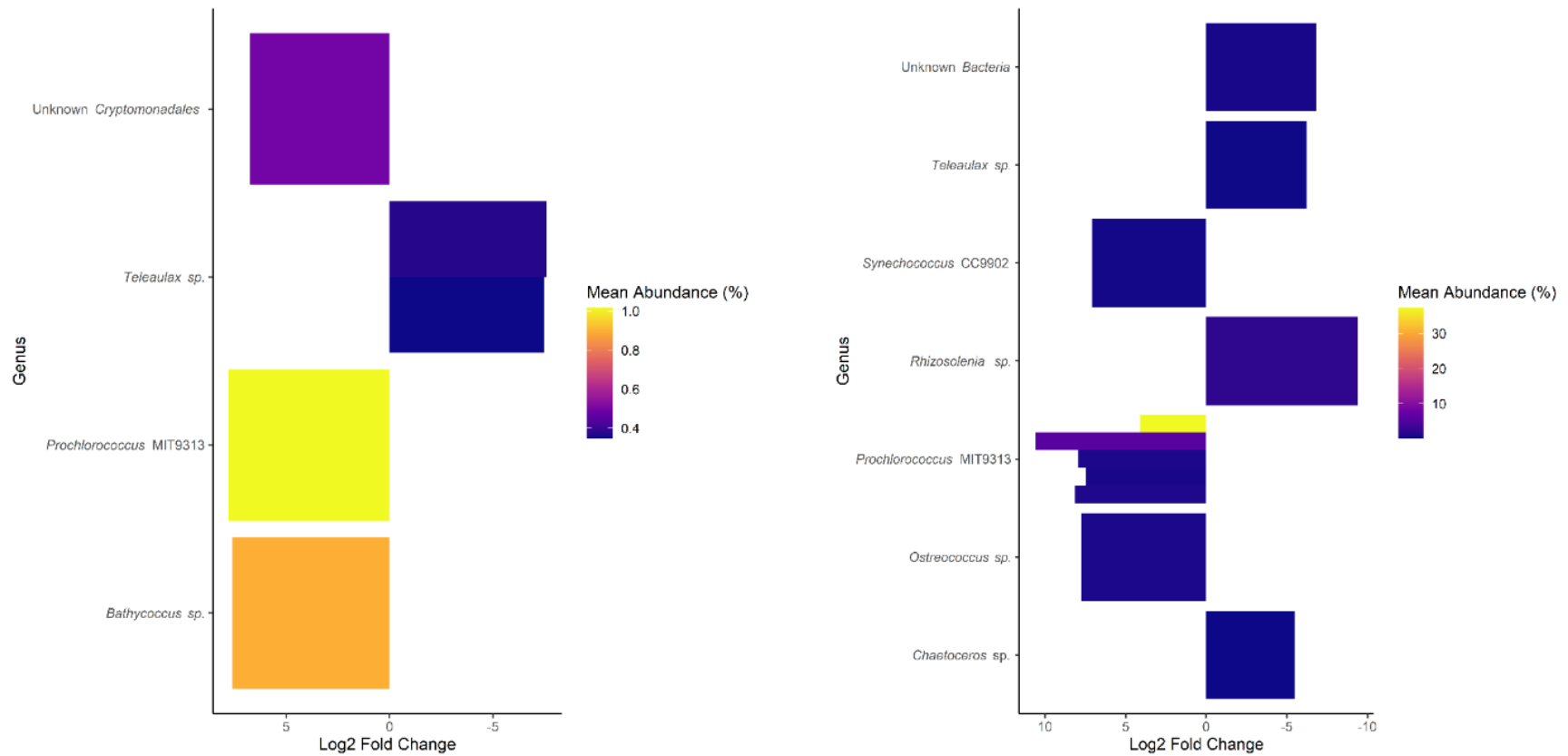


Figure 12: Difference in abundance of photoautotrophs expressed as significant (FDR, $p < 0.05$) fold change between normalized taxonomic counts in seawater (positive values) and trap material (negative values) from the (A) spring and (B) summer seasons. The color represents the average abundance of mean normalized counts in all samples.